Pergamon

J. Mech. Phys. Solids, Vol. 46, No. 12, pp. 2323–2359, 1998

Printed in Great Britain
0022–5096/98 $—see front matter

PII: S0022–5096(98)00008–8

KINETICS OF PHASE BOUNDARIES WITH EDGES AND JUNCTIONS

N. K. SIMHA* and K. BHATTACHARYA†‡

*Department of Mechanical Engineering, University of Miami, P.O. Box 248294, Coral Gables FL 33124-0642, U.S.A. †Division of Engineering and Applied Science, Mail Stop 104-44, California Institute of Technology, Pasadena CA 91125, U.S.A.

(*Received* 11 *September* 1997; *in revised form* 7 *January* 1998)

ABSTRACT

In this paper we study the propagation of a phase boundary which meets the boundary of the body at an edge or meets other phase boundaries at a junction. We show that it is necessary to provide kinetic relations for the edges and junctions in addition to the kinetic relation of the phase boundary. We derive thermodynamically consistent forms for these additional kinetic relations and show that they have a profound effect on the evolution of the phase boundary. © 1998 Elsevier Science Ltd. All rights reserved.

Keywords: A. phase boundary propagation, shape-memory effect, grain growth, contact angle, stress concentration.

1. INTRODUCTION

The evolution of microstructure is a crucial issue in a variety of phenomena like martensitic phase transformation, recrystallization and grain growth, solidification as well as the growth of thin films. Therefore, the propagation of interfaces or phase-boundaries has been widely studied (see Mullins 1956; Truskinovsky, 1987; Abeyaratne and Knowles, 1990; Gurtin, 1995; and the references therein). Consider a portion of an interface isolated from the boundary of the body and other interfaces. The propagation of this portion of the interface is completely determined by the normal velocity and there are well-developed models for this situation. The idea is to identify a thermodynamic driving force on the interface and to relate this driving force to the normal velocity using a (constitutive) kinetic relation.

Now consider a situation when an interface meets the boundary of the body at an edge or meets other interfaces at a junction. Two issues arise here:

(1) **Additional information.** The normal velocity alone does not determine the com-

‡To whom correspondence should be addressed. Fax: 001 626 568 2719. E-mail: bhatta@cco.caltech.edu.

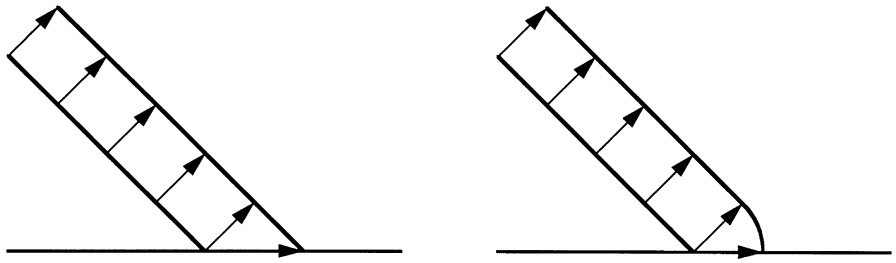

Fig. 1. Two interfaces with same initial conditions and same constant normal velocity evolve differently due to the edge.

plete evolution. Figure 1 shows two interfaces with identical initial position and propagating with identical (constant) normal velocity; yet they evolve differently. Clearly, additional information is necessary to ensure a unique solution. Similar additional information is also necessary at junctions (Taylor, 1995; Reitich and Soner, 1996).

(2) **Singularity.** The elastic moduli of the different phases can be different. Consequently, the stress and strain can be singular at an edge or a junction. It is possible that the singularity also plays a significant role in determining the kinetics of the edge or junction and consequently of the entire interface. Recall that it is the elastic singularity that provides the driving force for crack propagation in linear elastic fracture mechanics.

Figure 2 which shows the experimental observation of Chiao and Chen (1990) highlights the effect of the edge. This figure is a superposition of two transmission electron micrographs taken 10 s apart and it shows the propagation of an interface that separates the orthorhombic and monoclinic phases of zirconia (ZrO_2). Notice that the interface is bent near the edge where it meets the physical boundary of the body (encircled region).

In this paper, we study the kinetics of edges and multiple junctions in the presence of anisotropic interface energy and, possibly, singular elastic fields. We confine ourselves to two dimensions. In a sequel (Simha *et al.*, 1998), we generalize the results to three dimensions.

The issue of additional information at the edge or the triple junction has been discussed in the setting of interface-driven growth. Typically, the additional information is provided in the form of an equilibrium condition (see, for example, Murr, 1975). The oldest and best known of these is the Young's wetting angle condition or Herring condition which is relevant for a situation characterized by isotropic interface energy and constant bulk energy. Here, the balance of surface tensions fixes the angles between the different interfaces. In Fig. 1, it provides a limiting contact or edge angle, and this delivers uniqueness.

The use of such equilibrium contact conditions may solve the problem of non-uniqueness; yet it is not completely satisfactory. Notice that the interface propagates exactly when it is not at equilibrium. Yet the contact condition forces the edges to be

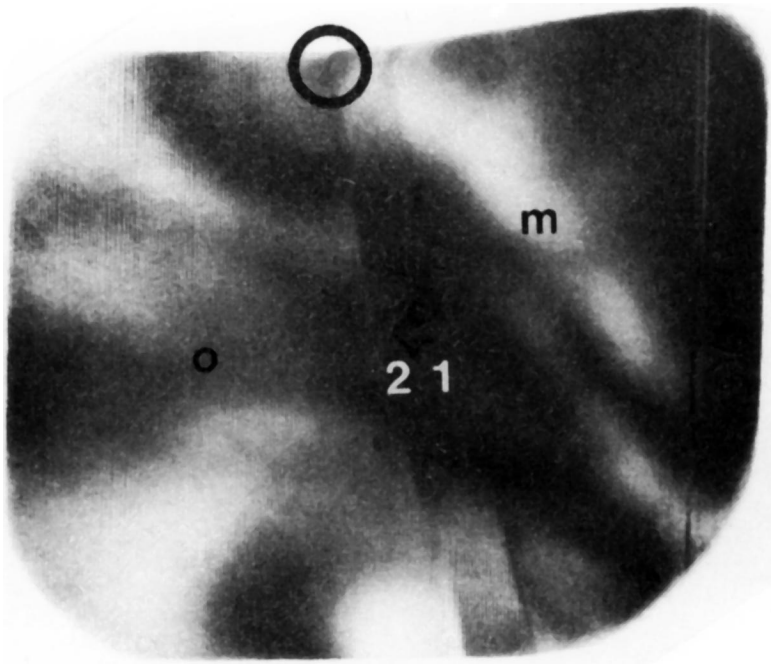

Fig. 2. The effect of the edge on a propagating interface that separates the orthorhombic and monoclinic phases of zirconia (ZrO_2). The interface bends away from the interior orientation at the top edge. The figure is a double exposure TEM taken 10 s apart. Reprinted from Y.-H. Chiao and I.-Wei Chen, *Acta Metallurgica et Materialia*, **38,** pp. 1163–1174, Copyright 1990 with the kind permission of the authors and Elsevier Science Ltd., The Boulevard, Langford Lane, Kidlington, OX51GB, U.K.

in equilibrium! There are experimental observations which show that this equilibrium condition may be violated. Studying the fluid flow through a capillary, Hoffman (1975) found that the contact angle changes with the velocity. Based on his experiments, a kinetic relation between the contact angle and the velocity of the contact line (edge) has been used in a variety of solid/fluid contact problems (Davis, 1983). We discuss this in Section 2.1. Angenent and Gurtin (1996) have derived a general kinetic relation in the presence of anisotropic interface energy and have also established some existence results.

The issue of kinetics of the edge or junction is very important in the study of martensitic phase transformation and the shape-memory effect. Hysteresis is a critical issue in these materials and phase boundary propagation is a source of the hysteresis—the interface dissipates energy as it propagates. Therefore it is important to understand the effect of the edges and junctions on the kinetics and also to understand their contribution to dissipation and hysteresis. Further, the edge raises important difficulties in the design of systematic experiments. This is explained in Section 2.2. We also study the nature of the singularity at an edge in this subsection. We find that in the setting of linear elasticity, the order of the singularity is completely determined by the elastic moduli and the local geometry. Gurtin and Voorhees (1998) considered

the effect of stress on the motion of faceted interfaces, but they restricted themselves to a special class of singularities that have no contribution to the kinetics.

Our main result is derived in Section 4. We examine the junction shown in Fig. 3 and calculate the dissipation associated with its motion. The dissipation is of the form

$$\mathbf{d}_J \cdot \mathbf{v}_J \tag{1.1}$$

where $\mathbf{v}_J$ is the velocity of the junction. Therefore, we call $\mathbf{d}_J$ the driving force acting on the junction. The driving force can be written as a sum of $(k+1)$ forces (4.49): one from each of the k interfaces and a final one from the elastic singularity. The contribution of the elastic singularity can be written as

$$\lim_{r\to 0} \int_{\partial \mathscr{B}_r} (\phi \mathbf{I} - \mathbf{F}^T \mathbf{S}) \hat{\mathbf{m}} \, \mathrm{d}l \tag{1.2}$$

where $\mathscr{B}_r$ is a disk of radius r centered at the junction, ϕ is the bulk free energy density, $\mathbf{F}$ is the deformation gradient, $\mathbf{S}$ is the (Piola–Kirchhoff) stress, and $\hat{\mathbf{m}}$ is the outward normal to $\partial \mathscr{B}_r$. Notice that this is reminiscent of the "J-integral" of fracture mechanics. We then propose a kinetic relation that relates the velocity of the junction to its driving force. Results for an edge are obtained as a special case of the junction. In Section 6 we state without discussion the generalization of this result to three dimensions.

We explore the implications of our result by studying various examples in Section 5. Section 5.1. studies interface driven phase boundary propagation: we assume that the bulk energy is constant in each phase. In particular, we study at length an example involving the propagation of an isotropic interface near an edge. It shows that the prescribed kinetic relation has a profound effect on the overall evolution of the interface. In fact, it affects both the overall velocity and the profile of the interface.

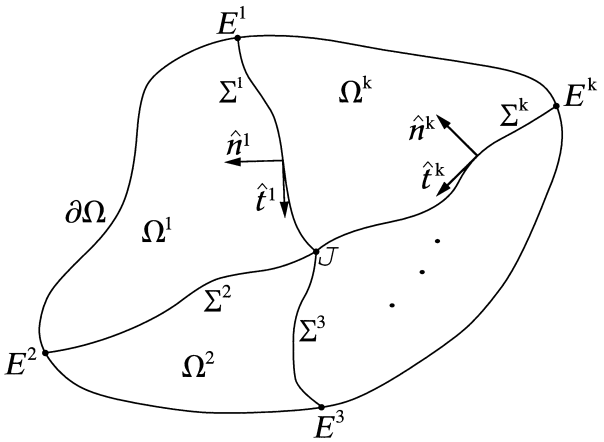

Fig. 3. A body Ω containing k interfaces. The interfaces intersect with each other at the junction J and with the external boundary $\partial\Omega$ at the edges E^i. The normal to an interface Σ^i is $\hat{\mathbf{n}}^i$ and the tangent is $\hat{\mathbf{t}}^i$. Arc-lengths increase from the edges to the junction.

Section 5.2 studies interface propagation in purely elastic multiphase bodies: we neglect all surface effects. The kinetics of the edge or junction is now completely guided by the *J*-type integral (1.2). We show that in the setting of linear elasticity, the driving force at an edge is finite only at some special contact or edge angles; it is either zero or infinite otherwise. It is finite at exactly those angles where the stress has a square-root singularity; it is zero if the singularity is weaker and infinite if the singularity is stronger. Now, if the edge kinetic relation forces the edge velocity to be unbounded for unbounded driving force, then the edge angle of a propagating interface necessarily takes these special values. Notice that this kinetic edge angle does not come from equilibrium. Thus, the elastic singularity can be important in determining the edge kinetics and consequently the interface evolution. We believe that this result may have similar implications for grain growth, thin film growth, etc. Therefore, we propose a design of an experiment on propagating interfaces that can separate the kinetics of the interior and that of the edge.

A reader primarily interested in interface driven propagation is encouraged to first read Subsections 2.1 and 5.1. A reader primarily interested in bulk driven propagation is encouraged to read Subsections 2.2 and 5.2.

As mentioned earlier, we infer the driving force in Section 4 by calculating the dissipation. In order to do so, we use the conceptual framework developed by Gurtin (1995). The concept of a configurational force is central to this framework, and it is very useful for studying phenomena such as the propagation of phase boundaries that involve changes in the reference configuration. Notice that a phase boundary is not a material surface. It separates parts of the body that are in different phases; hence as material transforms from one phase to another, the phase boundary moves relative to the particles of the body. Hence, phase boundary propagation results from a change in the reference configuration. We may interpret configurational forces as internal forces conjugate to the kinematic variables that describe changes in the reference configuration. They perform work on reference velocities and satisfy their own balance laws. We introduce and explain these concepts in Section 3, which draws completely from Gurtin (1995), by considering the familiar (and trivial) case of a single-phase elastic body.

Finally, we mention that it is also possible to infer these driving forces from a variational argument (Simha and Bhattacharya, 1997).

2. EXAMPLES

2.1. *Contact lines in fluid/solid systems*

We describe experiments that illustrate the effect of edges on interface propagation in fluid/solid systems. Figure 4(a) shows the experiment of Hoffman (1975). A fluid in a capillary forms a meniscus with air. At rest, the contact angle β is given by Young's wetting angle formula

$$\cos\beta = \frac{[\![\gamma]\!]}{\psi} \tag{2.1}$$

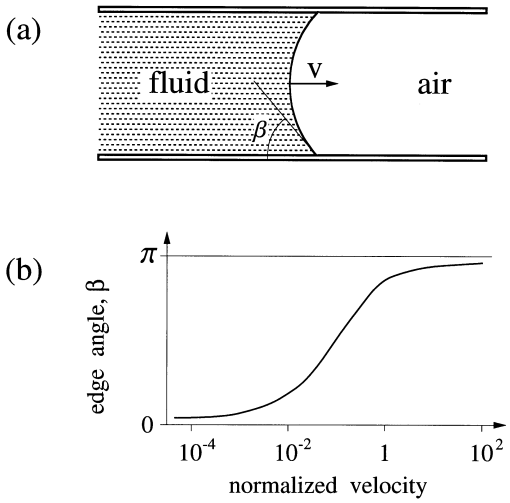

Fig. 4. (a) The fluid/air interface inside a capillary and its edge (contact) angle β. (b) When the fluid is forced with a piston, the edge angle changes with velocity (Hoffman, 1975) as shown schematically.

where ψ is the interface energy of the fluid/air interface and $[\![\gamma]\!]$ denotes the difference in the interface energy between the wet and dry wall. When the fluid was forced with a piston, Hoffman (1975) found that the contact angle changed with the velocity. Figure 4(b) is a schematic of his observations. Thus the dynamic edge angle can be vastly different from the stationary value given by (2.1).

Davis (1983) has catalogued various examples where the dependence of the contact angle on the edge velocity plays an important role; they include (i) the swelling of a liquid die when it exists a confining die into an empty chamber, (ii) a gas bubble rising in a liquid with surfactant islands on the gas/liquid interface, (iii) spreading of liquid drops on a plate, and (iv) solidification of a drop of melt on a crystal (Anderson and Davis, 1995).

2.2. *Martensitic phase transformation*

The kinetics of phase boundaries has been studied quite extensively in the context of martensitic phase transformation both theoretically and experimentally. However, it has proven to be difficult to connect these two : the theory is mainly one-dimensional while it is hard to design an essentially one dimensional experiment. At the same time, interpretation of the data in higher dimensional experiments is complicated. Much of the difficulty is related to edges.

Let us consider a simple experiment. A cylindrical single crystal specimen (with arbitrary cross-section) contains a single interface that separates two phases, e.g., a twin boundary separating two martensite variants. The lateral sides of the specimen are traction-free while the ends are subjected to dead tensile traction $\sigma\hat{\mathbf{a}}$. Here $\hat{\mathbf{a}}$ is the unit vector along the axis of the cylinder in the reference configuration and σ is the magnitude of the loading. If the phase boundary is not parallel to the axis, we expect

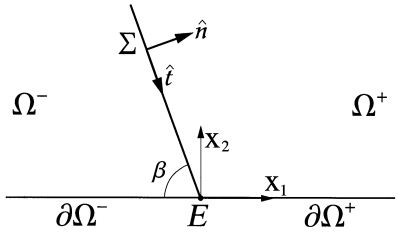

Fig. 5. The phase boundary Σ separates the upper half-plane into two regions Ω^+ and Ω^-. The normal to the interface is $\hat{\mathbf{n}}$ and the tangent is $\hat{\mathbf{t}}$. The (fixed) physical boundary of the body consists of $\partial\Omega^+$ and $\partial\Omega^-$, and the physical and phase boundaries intersect at the edge E.

the phase boundary to propagate as we change σ. We wish to measure the velocity of the interface as a function of the driving force it experiences. In order to interpret the results, it would be beneficial if the deformation gradient was piecewise constant and if the interface was a plane. Pitteri (1988) has shown that such a piecewise constant solution does not exist for a twin or austenite–martensite interface.

We briefly summarize his argument, which is by contradiction. Assume that the deformation gradient is piecewise constant with values $\mathbf{F}^+(\sigma)$ and $\mathbf{F}^-(\sigma)$. The Hadamard compatibility condition requires

$$\mathbf{F}^+(\sigma) - \mathbf{F}^-(\sigma) = \mathbf{b}(\sigma) \otimes \hat{\mathbf{n}}(\sigma) \tag{2.2}$$

for some nonzero vector $\mathbf{b}$ and where $\hat{\mathbf{n}}$ is the normal to the interface in the reference. The boundary conditions (applied loads at the ends and the traction-free lateral surface) imply that the Piola–Kirchhoff stress is constant and uniaxial, i.e.,

$$\mathbf{S} = \sigma \hat{\mathbf{a}} \otimes \hat{\mathbf{a}}. \tag{2.3}$$

Then, the symmetry of the Cauchy stress, traction continuity across the interface, and (2.2) imply that

$$\mathbf{F}^+ \hat{\mathbf{a}} \parallel \mathbf{F}^- \hat{\mathbf{a}} \parallel \hat{\mathbf{a}} \parallel \mathbf{b}. \tag{2.4}$$

This means that the deformed cylinder axis in the two phases and the shear $\mathbf{b}$ in the Hadamard condition (2.2) are parallel to the undeformed cylinder-axis. Notice that (2.4) holds for all values of the imposed load σ, and hence for $\sigma = 0$ by continuity. Finally, let us assume that

$$\det \mathbf{F}^+(0) = \det \mathbf{F}^-(0). \tag{2.5}$$

This condition is satisfied by twins (due to symmetry) and also by most shape-memory alloys for an austenite–martensite interface. Now (2.2), (2.4), and (2.5) imply that $\hat{\mathbf{a}} \cdot \hat{\mathbf{n}}(0) = 0$, which contradicts the requirement that the interface is not parallel to the cylinder-axis. Thus, it is not possible to have a piecewise constant solution.

The contradiction in the previous argument arises from two incompatible requirements—the traction-free lateral surface and traction continuity along the interface—at the edge. This incompatibility may lead to singular stresses at the edge. We elaborate on this issue by considering a simple problem in antiplane shear.

Consider the body shown in Fig. 5 that lies in the upper-half ($x_2 \geqslant 0$) of the x_1–x_2

plane. The planar interface Σ separates the body into two disjoint regions, Ω^+ and Ω^-. It meets the boundary of the body $\partial\Omega$ at the edge E. The region Ω^+ is occupied by material in the "$+$" phase, while the region Ω^- contains material in the "$-$" phase.

Let the out-of-plane component of the displacement be $u_3 = u(x_1, x_2)$. The only relevant strain and stress components are

$$\nabla u = \{u_{,1}, u_{,2}\} \quad \text{and} \quad \boldsymbol{\sigma} = \{\sigma_1, \sigma_2\} \tag{2.6}$$

where σ_1 is the 31-component and σ_2 the 32-component of the full three-dimensional stress tensor.

Assume that the $+$ phase has a stress-free strain or transformation strain $\{1, 1\}$, while the $-$ phase has a transformation strain $\{-1, -1\}$. Finally, let us assume that both phases are linearly elastic, so the stress–strain relations for the $\pm$ phases are

$$\begin{bmatrix} \sigma_1 \\ \sigma_2 \end{bmatrix} = \begin{bmatrix} a^\pm & c^\pm \\ c^\pm & b^\pm \end{bmatrix} \begin{bmatrix} u_{,1} \mp 1 \\ u_{,2} \mp 1 \end{bmatrix}. \tag{2.7}$$

We have assumed that the elastic moduli are anisotropic and different in the two phases; isotropy corresponds to $a^\pm = b^\pm$, $c^\pm = 0$. Clearly, we expect the elastic moduli to be different for the austenite and martensite phases. They are also different for two variants of martensite: though crystallographically equivalent, the variants are oriented differently.

Suppose the half-plane is subjected to the stress $\boldsymbol{\sigma} = \{\sigma^\infty, 0\}$ at infinity. The relevant equations are

$$\begin{aligned} \nabla \cdot \boldsymbol{\sigma} = \sigma_{1,1} + \sigma_{2,2} = 0 \quad & \text{in the regions } \Omega^\pm, \\ [\![\nabla u]\!] \cdot \hat{\mathbf{t}} = 0 \quad & \text{on the interface } \Sigma, \\ [\![\boldsymbol{\sigma}]\!] \cdot \hat{\mathbf{n}} = 0 \quad & \text{on the interface } \Sigma, \\ \sigma_2 = 0 \quad & \text{on the boundary } \partial\Omega^\pm, \\ \sigma_1 \to \sigma^\infty \quad & \text{as } x_1 \to \pm\infty; \end{aligned} \tag{2.8}$$

where $[\![a]\!]$ denotes the jump across the interface of the quantity a. The stress field satisfies the equilibrium equation $(2.8)_1$. Coherency is guaranteed by the perfect bond conditions—displacement continuity $(2.8)_2$ and traction continuity $(2.8)_3$—on the interface Σ. Equation $(2.8)_4$ is the traction-free boundary condition on the lower interface, while $(2.8)_5$ is the far-field boundary condition. Substituting (2.7) into (2.8) we obtain a set of equations for a single scalar unknown u.

We now want to show that the solution to the equations (2.8) is possibly singular at the edge E. We can do so by looking for an asymptotic solution near E. However, the situation becomes clearer by splitting the problem into two using the following superposition

$$u = v + w \tag{2.9}$$

where v satisfies the *auxiliary* problem:

$$
\begin{aligned}
a^{\pm}v_{,11}+2c^{\pm}v_{,12}+b^{\pm}v_{,22} &= 0 \quad \text{in } \Omega^{\pm},\\
[\![v_{,1}]\!]n_2-[\![v_{,2}]\!]n_1 &= 0 \quad \text{on } \Sigma,\\
[\![av_{,1}+cv_{,2}]\!]n_1+[\![cv_{,1}+bv_{,2}]\!]n_2 &= 2(\langle a+c\rangle n_1+\langle c+b\rangle n_2) \quad \text{on } \Sigma,\\
c^{\pm}v_{,1}+b^{\pm}v_{,2} &= \pm(c^{\pm}+b^{\pm}) \quad \text{on } \partial\Omega^{\pm}\,; \qquad (2.10)
\end{aligned}
$$

and w satisfies the *bi-material* problem:

$$
\begin{aligned}
a^{\pm}w_{,11}+2c^{\pm}w_{,12}+b^{\pm}w_{,22} &= 0 \quad \text{in } \Omega^{\pm},\\
[\![w_{,1}]\!]n_2-[\![w_{,2}]\!]n_1 &= 0 \quad \text{on } \Sigma,\\
[\![aw_{,1}+cw_{,2}]\!]n_1+[\![cw_{,1}+bw_{,2}]\!]n_2 &= 0 \quad \text{on } \Sigma,\\
c^{\pm}w_{,1}+b^{\pm}w_{,2} &= 0 \quad \text{on } \partial\Omega^{\pm},\\
a^{\pm}(w_{,1}\mp 1)+c^{\pm}(w_{,2}\mp 1) &\to \sigma^{\infty}-(a^{\pm}v_{,1}+c^{\pm}v_{,2}) \quad x_1\to\pm\infty. \qquad (2.11)
\end{aligned}
$$

Auxiliary problem. Let us examine if it is possible to find a piecewise linear solution. The first equation $(2.10)_1$ is then automatically satisfied and we are left with four linear equations for the four unknowns, $v^{+}_{,1}$, $v^{+}_{,2}$, $v^{-}_{,1}$, $v^{-}_{,2}$. The coefficients depend on the elastic moduli and the normal. We can solve these equations if

$$
\begin{aligned}
n_1(n_1(&-a^{+}b^{+}c^{-}+a^{-}b^{-}c^{+}+c^{+}c^{-}(c^{+}-c^{-}))\\
&+n_2(-b^{+}b^{-}(a^{+}-a^{-})-b^{+}(c^{-})^2+b^{-}(c^{+})^2))\neq 0. \qquad (2.12)
\end{aligned}
$$

Therefore, for generic values of the elastic moduli and normal, we can obtain a piecewise linear solution to (2.10).

For isolated choices of the normal and/or elastic moduli, the condition (2.12) is violated. Then, one finds a wide range of behavior. We do not present an exhaustive study, but it is interesting to look at two examples. First, consider the case when $n_1=0$. For this case we can find a one parameter family of piecewise linear solutions. Second, consider the case $a^{\pm}=b^{\pm}$, $c^{\pm}=0$, and $n_2=0$. Then, it is possible to show that the solution is singular at the edge.

Bimaterial problem. This is the well-known problem of the interface between two distinct elastic materials meeting a traction-free boundary (see for example Williams, 1952; Bogy, 1968; Kondratiev, 1967; Nicaise and Sändig, 1994; and the references therein). When subjected to far-field loads, it is possible that the material develops a singularity at the edge. While the precise solution depends on the applied loads, the order of the singularity does not: it depends only on the contact angle and the elastic moduli $(a^{\pm}, b^{\pm}, c^{\pm})$. In fact, one can determine the order of the singularity by looking asymptotically for a solution of the form $w=r^{\mu}f(\theta)$ in polar coordinates. Substituting this in (2.11) gives an eigenvalue problem with eigenvalue μ. In order to have finite energy, we retain only those eigenvalues with $\mu>0$. Notice that if $0\leqslant\mu_1<1$ (where μ_1 is the smallest positive eigenvalue), then the strain and consequently the stress is singular and the order of the singularity is (μ_1-1). Thus, the elastic moduli and the geometry completely determine whether the stress and the strain are singular, and if

so the order of the singularity. We refer the reader to Leguillon and Sanchez-Palencia (1987) (Theorem V.2.1) for the details in the case of anti-plane shear.

In conclusion, in the setting of antiplane shear, it is possible that the stress is singular at the edge. Except for some isolated values of the elastic moduli and interface orientation, the order of the singularity is exactly the same as one obtains at the junction between a bimaterial interface and a traction-free boundary. The elastic moduli of the two phases and the angle between the phase boundary and the boundary of the body completely determines if there is a singularity and also the order of the singularity.

Lastly, we get similar conclusions in plane strain. We can easily write down the analogs of eqns (2.7) and (2.8), and split them into auxiliary and bimaterial problems. The auxiliary problem has piecewise linear solutions (for generic values of the elastic moduli and geometry) and the bimaterial problem possibly has singular solutions.

3. CONFIGURATIONAL FORCES IN A SINGLE PHASE BODY

We introduce Gurtin's notion of configurational forces (Gurtin, 1995) using a single-phase material as an example. We write down the balance laws, calculate the dissipation, and obtain restrictions on constitutive equations using the second law of thermodynamics.

Let $\Omega \subset \mathbb{R}^2$ be the region occupied by a single-phase material in the reference configuration. We denote the deformation by $\mathbf{y}$; the deformation gradient is $\mathbf{F}$, and the material velocity is $\dot{\mathbf{y}}$. We introduce two sets of forces and stresses. The first are the classical forces and stresses; we call these deformational. So, the deformational stress is the classical Piola–Kirchhoff stress $\mathbf{S}$. We ignore deformational body forces like gravity for convenience. The second set of forces and stresses are configurational. As explained in the introduction, these are conjugate to changes in the reference configuration. We consider an external configurational body force $\mathbf{f}$ and a configurational bulk stress $\mathbf{C}$. In this section, we assume that all quantities are sufficiently smooth in Ω.

3.1. *Balance laws*

The standard balance of deformational forces and moments are

$$\int_{\partial \mathscr{D}_t} \mathbf{S}\hat{\mathbf{m}}\, \mathrm{d}l = 0 \quad \text{and} \quad \int_{\partial \mathscr{D}_t} \mathbf{y} \times \mathbf{S}\hat{\mathbf{m}}\, \mathrm{d}l = 0 \tag{3.1}$$

for every sub-region $\mathscr{D}_t \subset \Omega$ and for each time t. Localization of these balance laws using the divergence theorem gives

$$\nabla \cdot \mathbf{S} = 0; \quad \mathbf{S}\mathbf{F}^T = \mathbf{F}\mathbf{S}^T \quad \text{in } \Omega. \tag{3.2}$$

Configurational forces satisfy the force balance

$$\int_{\mathscr{D}_t} \mathbf{f}\,\mathrm{d}a + \int_{\partial\mathscr{D}_t} \mathbf{C}\hat{\mathbf{m}}\,\mathrm{d}l = 0, \tag{3.3}$$

for every $\mathscr{D}_t \subset \Omega$ and for all t. This localizes to

$$\nabla\cdot\mathbf{C} + \mathbf{f} = 0. \tag{3.4}$$

We omit the configurational moment balance since we will not need it; see Gurtin (1995).

3.2. *Dissipation inequality*

Let $\mathscr{D}_t$ be an evolving subregion of the reference domain Ω. Let $\hat{\mathbf{m}}$ be the external normal to the curve $\partial\mathscr{D}_t$, and suppose that the curve $\partial\mathscr{D}_t$ is described by the parametrization

$$\partial\mathscr{D}_t = \{\mathbf{x}\in\Omega : \mathbf{x} = \tilde{\mathbf{x}}(\delta, t)\} \tag{3.5}$$

where δ is a scalar parameter and t denotes the time. The velocity of the curve and its normal component can be calculated as

$$\mathbf{u} = \frac{\partial\tilde{\mathbf{x}}(\cdot, t)}{\partial t} \quad \text{and} \quad u_m = \mathbf{u}\cdot\hat{\mathbf{m}}. \tag{3.6}$$

However, only the normal component u_m of the curve velocity is independent of the parameterization. The deformation maps the curve $\partial\mathscr{D}_t$ to a curve $\mathbf{y}(\partial\mathscr{D}_t)$ in the deformed configuration, and the velocity field of $\mathbf{y}(\partial\mathscr{D}_t)$ is

$$\frac{\partial\mathbf{y}(\tilde{\mathbf{x}}(\cdot, t), t)}{\partial t} = \dot{\mathbf{y}} + \mathbf{F}\mathbf{u}. \tag{3.7}$$

Working. The important difference between the deformational and configurational forces is their conjugate velocities: deformational forces are conjugate to the velocity in the deformed configuration while configurational forces are conjugate to the velocity in the reference configuration. Thus, the external working on the region $\mathscr{D}_t$ is

$$\mathscr{W}(\mathscr{D}_t) = \int_{\partial\mathscr{D}_t} [\mathbf{S}\hat{\mathbf{m}}\cdot(\dot{\mathbf{y}} + \mathbf{F}\mathbf{u}) + \mathbf{C}\hat{\mathbf{m}}\cdot\mathbf{u}]\,\mathrm{d}l. \tag{3.8}$$

The configurational force $\mathbf{f}$ does not perform any work since points in the interior of the region $\mathscr{D}_t$ are stationary in the reference.

The working (3.8) is required to be independent of parameterizations of the curve $\partial\mathscr{D}_t$. Since only the normal component of the curve velocity u_m is independent of the parameterization (3.5), it is necessary that

$$(\mathbf{F}^T\mathbf{S} + \mathbf{C})\hat{\mathbf{m}}\cdot\hat{\mathbf{t}} = 0 \tag{3.9}$$

where $\hat{\mathbf{t}}$ denotes the tangent to the curve $\partial\mathscr{D}_t$. Now, this relation should hold for any region $\mathscr{D}_t \subset \Omega$. In other words, (3.9) is true for every pair of mutually perpendicular vectors $\hat{\mathbf{m}}$ and $\hat{\mathbf{t}}$. It follows that $(\mathbf{F}^T\mathbf{S} + \mathbf{C})\hat{\mathbf{m}}$ is parallel to $\hat{\mathbf{m}}$ and we obtain

$$\mathbf{C} = \pi\mathbf{I} - \mathbf{F}^T\mathbf{S} \tag{3.10}$$

for some scalar field π and where $\mathbf{I}$ denotes the identity.

Energy. Let the bulk energy per unit reference area be ϕ. Then the energy of the region $\mathscr{D}_t$ is

$$\mathscr{E}(\mathscr{D}_t) = \int_{\mathscr{D}_t} \phi \, \mathrm{d}a, \tag{3.11}$$

and we get

$$\frac{\mathrm{d}\mathscr{E}(\mathscr{D}_t)}{\mathrm{d}t} = \int_{\mathscr{D}_t} \dot{\phi} \, \mathrm{d}a + \int_{\partial\mathscr{D}_t} \phi u_m \, \mathrm{d}l \tag{3.12}$$

since the region $\mathscr{D}_t$ depends on time.

Dissipation inequality. The dissipation Γ of the region $\mathscr{D}_t$ is defined as

$$\Gamma(\mathscr{D}_t) = \mathscr{W}(\mathscr{D}_t) - \frac{\mathrm{d}\mathscr{E}(\mathscr{D}_t)}{\mathrm{d}t}. \tag{3.13}$$

The appropriate mechanical version of the Clausius–Duhem inequality or the second law of thermodynamics requires the dissipation Γ to be non-negative, i.e.,

$$\Gamma(\mathscr{D}_t) \geqslant 0 \quad \text{for every } \mathscr{D}_t \subset \Omega. \tag{3.14}$$

Using equations (3.8), (3.10), and (3.12) in (3.13) we can write the dissipation as

$$\Gamma(\mathscr{D}_t) = -\int_{\mathscr{D}_t} \dot{\phi} \, \mathrm{d}a + \int_{\partial\mathscr{D}_t} [\mathbf{S}\hat{\mathbf{m}} \cdot \dot{\mathbf{y}} + (\pi - \phi)u_m] \, \mathrm{d}l.$$

Using the divergence theorem and the localized version of the balance of forces (3.2), we get

$$\Gamma(\mathscr{D}_t) = \int_{\mathscr{D}_t} [\mathbf{S} \cdot \dot{\mathbf{F}} - \dot{\phi}] \, \mathrm{d}a + \int_{\partial\mathscr{D}_t} (\pi - \phi)u_m \, \mathrm{d}l. \tag{3.15}$$

We can now use the dissipation inequality (3.14) to conclude that

$$\pi = \phi. \tag{3.16}$$

Consider a second region $\mathscr{D}'_t$ such that (i) it coincides with the region $\mathscr{D}_t$ at time t and (ii) the boundary $\partial\mathscr{D}'_t$ has a normal velocity $u'_m \neq u_m$. We obtain an expression similar to (3.15) for $\Gamma(\mathscr{D}'_t)$. The dissipation inequality (3.14) must be satisfied for both regions, which implies (3.16).

Consequently, the bulk configurational stress,

$$\mathbf{C} = \phi\mathbf{I} - \mathbf{F}^T\mathbf{S}, \tag{3.17}$$

from eqns (3.16) and (3.10). Thus the bulk configurational stress is nothing but the well-known Eshelby or Noether energy-momentum tensor.

Finally, upon using (3.16), the dissipation inequality (3.14) reduces to

$$\Gamma(\mathscr{D}_t) = \int_{\mathscr{D}_t} [\mathbf{S}\cdot\dot{\mathbf{F}} - \dot{\phi}]\, \mathrm{d}a \geqslant 0. \tag{3.18}$$

We can localize it to obtain

$$\Gamma_{\text{bulk}} = \mathbf{S}\cdot\dot{\mathbf{F}} - \dot{\phi} \geqslant 0. \tag{3.19}$$

Notice that the dissipation (3.18) agrees with the standard calculation that does not use configurational forces or evolving regions (Gurtin, 1981).

3.3. *Constitutive equations*

Let us now specialize to the case of elasticity by making the assumptions $\phi = \phi(\mathbf{F}, \mathbf{x})$ and $\mathbf{S} = \mathbf{S}(\mathbf{F}, \mathbf{x})$ where the dependence on $\mathbf{x} \in \Omega$ means the body is inhomogeneous. Substituting these in (3.19) and requiring that it hold for all deformations of the body, we conclude that

$$\mathbf{S} = \frac{\partial \phi}{\partial \mathbf{F}} \tag{3.20}$$

following the arguments of Coleman and Noll (1963). Consequently, the dissipation vanishes in the elastic material.

Finally, eqns (3.4) and (3.17) imply that the configurational body force is given by

$$\mathbf{f} = -\frac{\partial \phi}{\partial \mathbf{x}}. \tag{3.21}$$

Thus there is configurational body force whenever the body is inhomogeneous. This would provide the driving force if a transport mechanism that seeks to homogenize the body were present.

In conclusion, by introducing configurational forces and considering regions that evolve in the reference configuration, we not only recover the classical results (3.18) and (3.20), but obtain the additional insights (3.10) and (3.21).

4. KINETICS OF JUNCTIONS AND EDGES

Consider a body in its reference configuration $\Omega \in \mathbb{R}^2$; the body is divided into k (open) regions Ω^i, $i = 1, 2, \ldots, k$ by interfaces Σ^i, $i = 1, 2, \ldots, k$ that intersect at the junction J (see Fig. 3). The unit normal to the interface Σ_i (pointing into Ω^i) is $\hat{\mathbf{n}}^i$. We have in mind that the material in different regions are in different phases, hence the Σ^i are phase boundaries. In this section, we study the kinetics of the interfaces as well as those of the junction. We recover known results for an interface and find new results for the junction.

We note that edges are a special case of the junction. Consider the edge shown in Fig. 5. If we set $\Omega^+ = \Omega^1$, $\Omega^- = \Omega^2$, $\Sigma = \Sigma^1$, $\partial\Omega^- = \Sigma^2$, and $\partial\Omega^+ = \Sigma^3$ in Fig. 5, the edge E can now be regarded as a triple-junction in the notation of Fig. 3. The following discussion about junctions also applies for the edge, but with an important caveat. The interfaces Σ^2 and Σ^3 are fixed and hence the edge is constrained to move on the physical boundary. Thus, we treat an edge as a constrained junction.

4.1. *Kinematics*

Let us return to the junction shown in Fig. 3. Let the interface Σ^i be described by an arc-length parameterization

$$\Sigma^i(t) = \{\mathbf{x} \in \mathbb{R}^2 : \mathbf{x} = \bar{\mathbf{x}}^i(\alpha^i, t)\} \tag{4.1}$$

where the arc-length α^i increases from the edge E^i to the junction J. The (unit) tangent vector $\hat{\mathbf{t}}^i$ to the interface $\Sigma^i(t)$ points in the direction of increasing arc-length α^i and is obtained from

$$\hat{\mathbf{t}}^i = \frac{\partial \bar{\mathbf{x}}^i(\alpha^i, \cdot)}{\partial \alpha^i}; \quad |\hat{\mathbf{t}}^i| = 1. \tag{4.2}$$

The reference velocity of the interface $\mathbf{v}^i$ and its normal component v_n^i are given by

$$\mathbf{v}^i = \frac{\partial \bar{\mathbf{x}}^i(\cdot, t)}{\partial t} \quad \text{and} \quad v_n^i = \mathbf{v}^i \cdot \hat{\mathbf{n}}^i. \tag{4.3}$$

Only the normal component is independent of the parameterization (4.1) that we have chosen.

Let us now consider a deformation: $\mathbf{y} : \Omega \times T \to \mathbb{R}^2$ where T is a time interval. The deformation gradient $\mathbf{F}$ and material velocity $\dot{\mathbf{y}}$ are given by

$$\mathbf{F}(\mathbf{x}, \cdot) = \nabla \mathbf{y}(\mathbf{x}, \cdot) = \frac{\partial \mathbf{y}(\mathbf{x}, \cdot)}{\partial \mathbf{x}} \quad \text{and} \quad \dot{\mathbf{y}}(\cdot, t) = \frac{\partial \mathbf{y}(\cdot, t)}{\partial t}. \tag{4.4}$$

We are interested in coherent interfaces that separate regions containing material in different phases. Hence we assume that the deformation is continuous in the entire body Ω and smooth in each of the regions Ω^i. However, we allow the deformation gradient $\mathbf{F}$ and the material velocity $\dot{\mathbf{y}}$ to be discontinuous across the interfaces. This imposes the following compatibility conditions on Σ^i

$$[\![\mathbf{F}]\!] = [\![\mathbf{F}]\!]\hat{\mathbf{n}}^i \otimes \hat{\mathbf{n}}^i, \tag{4.5}$$

$$[\![\dot{\mathbf{y}}]\!] = -v_n^i [\![\mathbf{F}]\!]\hat{\mathbf{n}}^i. \tag{4.6}$$

Above, $[\![\mathbf{a}]\!] = (\mathbf{a}^+ - \mathbf{a}^-)$ denotes the jump across the interface and $\mathbf{a}^+(\mathbf{a}^-)$ is the limiting value of quantity $\mathbf{a}$ from the region $\Omega^i(\Omega^{i-1})$ at the interface Σ_i. [The first is the Hadamard jump condition and the second condition follows from (4.8).]

We now describe the deformation of the interface $\Sigma^i(t)$. By composing the bulk deformation $\mathbf{y}$ with the interface parameterization (4.1) we define

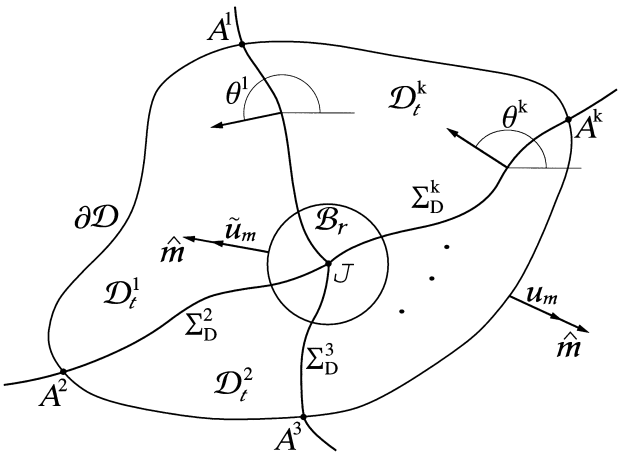

Fig. 6. A region $\mathscr{D}_t \subset \Omega$ that contains the junction J. Its boundary $\partial\mathscr{D}_t$ intersects the interfaces at points A^i; the boundary moves with a normal velocity u_m. The disk $\mathscr{B}_r$ of radius r is centered at the junction, and its boundary $\partial\mathscr{B}_r$ moves with a normal velocity $\tilde{u}_m$. The normals to both surfaces $\partial\mathscr{D}_t$ and $\partial\mathscr{B}_r$ are denoted as $\hat{\mathbf{m}}$. The part of the interface Σ^i within the sub-body $\mathscr{D}_t$ is Σ_D^i.

$$\bar{\mathbf{y}}^i(\alpha^i, t) = \mathbf{y}^+(\bar{\mathbf{x}}^i(\alpha^i, t), t) = \mathbf{y}^-(\bar{\mathbf{x}}^i(\alpha^i, t), t). \tag{4.7}$$

Differentiating eqn (4.7) with respect to t, the velocity of the interface in the current configuration is obtained as

$$\dot{\bar{\mathbf{y}}}^i = \frac{\partial \bar{\mathbf{y}}^i(\cdot, t)}{\partial t} = \dot{\mathbf{y}}^+ + \mathbf{F}^+\mathbf{v}^i = \dot{\mathbf{y}}^- + \mathbf{F}^-\mathbf{v}^i = \langle\dot{\mathbf{y}}\rangle + \langle\mathbf{F}\rangle\mathbf{v}^i \tag{4.8}$$

where the average across an interface is denoted as $\langle a\rangle = (a^+ + a^-)/2$. The deformation $\bar{\mathbf{y}}$ causes a tangential stretch $\mathbf{p}^i$ of the interface Σ^i where

$$\mathbf{p}^i = \frac{\partial \bar{\mathbf{y}}^i(\alpha^i, \cdot)}{\partial \alpha^i}. \tag{4.9}$$

For future use, we define the projection of the deformation gradients on the interface as

$$\bar{\mathbf{F}}^i = \mathbf{F}^{\pm}(\mathbf{I} - \hat{\mathbf{n}}^i \otimes \hat{\mathbf{n}}^i) = \langle\mathbf{F}\rangle(\mathbf{I} - \hat{\mathbf{n}}^i \otimes \hat{\mathbf{n}}^i). \tag{4.10}$$

The equalities follow from the compatibility condition (4.5). $\bar{\mathbf{F}}$ maps tangents to the interface in the reference configuration into tangents to the interface in the deformed configuration. The following identities relate the various interface quantities

$$\mathbf{p}^i = \bar{\mathbf{F}}^i\hat{\mathbf{t}}^i = \langle\mathbf{F}\rangle\hat{\mathbf{t}}^i; \quad \bar{\mathbf{F}}^i\hat{\mathbf{n}}^i = 0. \tag{4.11}$$

Finally, consider the junction J where the bulk fields may be singular. In classical potential theory, the standard procedure is to exclude a small region around the singular point. The required analysis is then performed in the punctured domain, and relevant equations are obtained in the limit as the region vanishes. Let $\mathscr{B}_r$ be a disk of radius $r > 0$ centered at the junction (see Fig. 6). The boundary of the disk $\partial\mathscr{B}_r$

Table 1. *Summary of forces and stresses*

Region	Deformational		Configurational	
	Force	Stress	Force	Stress
Bulk Ω^i	—	$\mathbf{S}$	$\mathbf{f}$	$\mathbf{C}$
Interface Σ^i	—	$\mathbf{s}^i$	$\mathbf{f}^i_\Sigma$	$\mathbf{c}^i$
Junction J	—	—	$\mathbf{f}_J$	—

has an outward normal $\hat{\mathbf{m}}$, velocity $\tilde{\mathbf{u}}$ in the reference configuration, and velocity $\dot{\mathbf{y}}+\mathbf{F}\tilde{\mathbf{u}}$ in the deformed configuration.

4.2. *Balance laws*

The forces and stresses that we consider are listed in Table 1. As before we assume that all deformational forces are contact forces. In Section 3 we have already encountered the bulk quantities: deformational (or classical Piola–Kirchhoff) stress $\mathbf{S}$, configurational stress $\mathbf{C}$, and configurational force $\mathbf{f}$. We take the bulk quantities to be smooth in each region Ω^i, however, they can suffer jumps across interfaces Σ^i and can be singular at the junction J. On each of the interfaces, we introduce a deformational stress $\mathbf{s}^i$, configurational stress $\mathbf{c}^i$ and configurational force $\mathbf{f}^i_\Sigma$. In two dimensions the interface is a curve, hence the stresses $\mathbf{s}^i$ and $\mathbf{c}^i$ are vectors; their action will be clear when we write balance laws. We assume that the interface quantities—$\mathbf{s}^i$, $\mathbf{c}^i$, and $\mathbf{f}^i_\Sigma$—are smooth on the interfaces Σ^i and are continuous up to the junction J. Finally, $\mathbf{f}_J$ is the configurational force that acts on the point J.

Consider an evolving region $\mathscr{D}_t \subset \Omega$ that contains the junction J as shown in Fig. 6. Its boundary is denoted by $\partial\mathscr{D}_t$, and the external normal to $\partial\mathscr{D}_t$ is the unit vector $\hat{\mathbf{m}}$. Let the part of the interface Σ^i that intersects with the subregion $\mathscr{D}_t$ be $\Sigma^i_D = \Sigma^i \bigcap \mathscr{D}_t$; its boundary consists of two points A^i (arc-length α^i_A) and the junction J.

The deformational contact forces arise from the bulk stress $\mathbf{S}$ acting on the boundary $\partial\mathscr{D}_t$ and interface stress $\mathbf{s}^i$ acting at points A^i. The balance of deformational forces requires that

$$\int_{\partial\mathscr{D}_t} \mathbf{S}\hat{\mathbf{m}}\,\mathrm{d}a - \sum_{i=1}^{k} \mathbf{s}^i|_{A^i} = 0 \tag{4.12}$$

for every $\mathscr{D}_t \subset \Omega$ and each time t. The symbol $\mathbf{a}^i|_{A^i}$ means that the quantity $\mathbf{a}^i$ is evaluated at the point A^i. The configurational contact forces arise from the bulk stress $\mathbf{C}$ acting on $\partial\mathscr{D}_t$, interface stresses $\mathbf{c}^i$ acting at points A^i, and the balance of configurational forces requires that

$$\int_{\mathscr{D}_t} \mathbf{f}\,\mathrm{d}a + \int_{\Sigma^i_D} \mathbf{f}^i_\Sigma\,\mathrm{d}l + \int_{\partial\mathscr{D}_t} \mathbf{C}\hat{\mathbf{m}}\,\mathrm{d}l - \sum_{i=1}^{k} \mathbf{c}^i|_{A^i} + \mathbf{f}_J = 0 \tag{4.13}$$

for every $\mathscr{D}_t \subset \Omega$ and each time t.

Since the bulk stresses can be singular at the junction, we need to be careful in localizing the balance laws (4.12) and (4.13). We remove a circle $\mathscr{B}_r$ of radius r centered at the junction, apply the usual divergence theorem in the domain $\mathscr{D}_t \backslash \mathscr{B}_r$ and then take the limit $r \to 0$. See eqns (A6) and (A8) in Appendix A for details.

We localize the deformational force balance (4.12) and obtain

$$\nabla \cdot \mathbf{S} = 0 \quad \text{in } \Omega^i, \tag{4.14}$$

$$[\![\mathbf{S}]\!]\hat{\mathbf{n}}^i + \frac{\partial \mathbf{s}^i}{\partial \alpha^i} = 0 \quad \text{in } \Sigma^i, \tag{4.15}$$

$$\lim_{r \to 0} \int_{\partial \mathscr{B}_r} \mathbf{S}\hat{\mathbf{m}} \, \mathrm{d}l - \sum_{i=1}^{k} \mathbf{s}^i|_J = 0 \quad \text{at } J. \tag{4.16}$$

Equation (4.14) in the bulk is the familiar equilibrium equation of continuum mechanics. On the interfaces, eqn (4.15) requires the jump in the bulk contact force to balance the tangential derivative or "surface divergence" of the interface stress. The limiting value of the singular bulk stress balances the interface contact stresses at the junction (4.16).

Note that $\mathbf{s}^i|_J$ may be infinite, so (4.16) appears to be a sum of infinite terms. However, it has the following meaning

$$\lim_{r \to 0} \left[\int_{\partial \mathscr{B}_r} \mathbf{S}\hat{\mathbf{m}} \, \mathrm{d}l - \sum_{i=1}^{k} \mathbf{s}^i|_{\Sigma^i_D \cap \partial \mathscr{B}_r} \right] = 0. \tag{4.17}$$

For simplicity of notation we continue to write (4.16), but we use it in the sense of (4.17) in this and other similar situations.

Localization of the configurational force balance (4.13) gives

$$\nabla \cdot \mathbf{C} + \mathbf{f} = 0 \quad \text{in } \Omega^i, \tag{4.18}$$

$$[\![\mathbf{C}]\!]\hat{\mathbf{n}}^i + \frac{\partial \mathbf{c}^i}{\partial \alpha^i} + \mathbf{f}^i_\Sigma = 0 \quad \text{in } \Sigma_i, \tag{4.19}$$

$$\lim_{r \to 0} \int_{\partial \mathscr{B}_r} \mathbf{C}\hat{\mathbf{m}} \, \mathrm{d}l - \sum_{i=1}^{k} \mathbf{c}^i|_J + \mathbf{f}_J = 0 \quad \text{at } J. \tag{4.20}$$

4.3. *Dissipation inequality*

In this subsection, we calculate the dissipation in the evolving region $\mathscr{D}_t$. First, we calculate the working (4.21), the rate of change of the stored energy (4.32), and the dissipation (4.35). We use the dissipation inequality or the second law of thermodynamics to deduce the configurational stresses to be (4.39) and (4.40). Finally the dissipation reduces to (4.45). This equation is used in Section 4.4 to identify the driving forces.

Working. Deformational forces perform work on the velocities in the deformed

configuration and configurational forces on the velocities in the reference. Thus, the external working on region $\mathscr{D}_t$ is

$$\mathscr{W}(\mathscr{D}_t) = \int_{\partial\mathscr{D}_t} [\mathbf{S}\hat{\mathbf{m}}\cdot(\dot{\mathbf{y}}+\mathbf{F}\mathbf{u}) + \mathbf{C}\hat{\mathbf{m}}\cdot\mathbf{u}]\,\mathrm{d}l - \sum_{i=1}^{k} [\mathbf{s}^i\cdot(\langle\dot{\mathbf{y}}\rangle + \langle\mathbf{F}\rangle\mathbf{v}_{A^i}) + \mathbf{c}^i\cdot\mathbf{v}_{A^i}]_{A^i}. \tag{4.21}$$

Above, $\mathbf{v}_{A^i}$ is the velocity of the intersection A^i in the reference configuration the velocities in the deformed configuration have been obtained from eqns (3.7) and (4.8).

The working (4.21) must be independent of parameterizations of the boundary $\partial\mathscr{D}_t$. Only the normal component u_m is independent of the parameterizations (3.5), hence condition (3.9) holds. This yields the representation (3.10) for the bulk configurational stress.

It is convenient to introduce the normal and tangential components of $\mathbf{c}^i + \langle\mathbf{F}\rangle^T\mathbf{s}^i$:

$$\mathbf{c}^i + \langle\mathbf{F}\rangle^T\mathbf{s}^i = \sigma^i\hat{\mathbf{t}}^i + \bar{\xi}^i\hat{\mathbf{n}}^i.$$

Then, using the identity $[(\bar{\mathbf{F}}^i)^T - \langle\mathbf{F}\rangle^T]\mathbf{s}^i = -(\langle\mathbf{F}\rangle\hat{\mathbf{n}}^i\cdot\mathbf{s}^i)\hat{\mathbf{n}}^i$, and setting $\xi^i = \bar{\xi}^i + (\langle\mathbf{F}\rangle\hat{\mathbf{n}}^i\cdot\mathbf{s}^i)$, we obtain

$$\mathbf{c}^i = \sigma^i\hat{\mathbf{t}}^i + \xi^i\hat{\mathbf{n}}^i - (\bar{\mathbf{F}}^i)^T\mathbf{s}^i. \tag{4.22}$$

This gives a representation for the configurational stress of an interface.

In the next few steps we will simplify the expression for the working (4.21); the final reduced form is (4.31). We split the working (4.21) into two parts as

$$\mathscr{W}_1 \overset{\text{def}}{=} \int_{\partial\mathscr{D}_t} [\mathbf{S}\hat{\mathbf{m}}\cdot\dot{\mathbf{y}} + (\mathbf{C}+\mathbf{F}^T\mathbf{S})\hat{\mathbf{m}}\cdot\mathbf{u}]\,\mathrm{d}l, \tag{4.23}$$

$$\mathscr{W}_2 \overset{\text{def}}{=} -\sum_{i=1}^{k} [\mathbf{s}^i\cdot\langle\dot{\mathbf{y}}\rangle + (\mathbf{c}^i + \langle\mathbf{F}\rangle^T\mathbf{s}^i)\cdot\mathbf{v}_{A^i}]_{A^i}. \tag{4.24}$$

By using the representation (3.10) for the bulk configurational stress $\mathbf{C}$, we rewite (4.23) as

$$\mathscr{W}_1 = \int_{\partial\mathscr{D}_t} \mathbf{S}\hat{\mathbf{m}}\cdot\dot{\mathbf{y}}\,\mathrm{d}l + \int_{\partial\mathscr{D}_t} \pi u_m\,\mathrm{d}l. \tag{4.25}$$

The divergence theorem (A6) then implies that

$$\mathscr{W}_1 = \int_{\partial\mathscr{D}_t} \pi u_m\,\mathrm{d}l + \int_{\mathscr{D}_t} \nabla\cdot(\mathbf{S}^T\dot{\mathbf{y}})\,\mathrm{d}a + \lim_{r\to 0}\int_{\partial\mathscr{B}_r} \mathbf{S}\hat{\mathbf{m}}\cdot\dot{\mathbf{y}}\,\mathrm{d}l + \sum_{i=1}^{k}\int_{\Sigma_D^i} [\langle\mathbf{S}\rangle\hat{\mathbf{n}}^i\cdot[\![\dot{\mathbf{y}}]\!] + [\![\mathbf{S}]\!]\hat{\mathbf{n}}^i\cdot\langle\dot{\mathbf{y}}\rangle]\,\mathrm{d}l. \tag{4.26}$$

Lastly, the identity $\nabla\cdot(\mathbf{S}^T\dot{\mathbf{y}}) = \dot{\mathbf{y}}\cdot(\nabla\cdot\mathbf{S}) + \mathbf{S}\cdot\dot{\mathbf{F}}$, the balance law (4.14), and the compatibility condition (4.6) imply that

$$\mathscr{W}_1 = \int_{\partial\mathscr{D}_t} \pi u_m \,\mathrm{d}l + \int_{\mathscr{D}_t} \mathbf{S}\cdot\dot{\mathbf{F}}\,\mathrm{d}a + \lim_{r\to 0}\int_{\partial\mathscr{B}_r} \mathbf{S}\hat{\mathbf{m}}\cdot\dot{\mathbf{y}}\,\mathrm{d}l + \sum_{i=1}^{k}\int_{\Sigma_D^i} [[\![\mathbf{S}]\!]\hat{\mathbf{n}}^i\cdot\langle\dot{\mathbf{y}}\rangle - \langle\mathbf{S}\rangle\hat{\mathbf{n}}^i\cdot[\![\mathbf{F}]\!]\hat{\mathbf{n}}^i v_n^i]\,\mathrm{d}l. \quad (4.27)$$

Next, using the representation (4.22) for the interface configurational stress $\mathbf{c}^i$, we rewrite $\mathscr{W}_2$ (2.24) as

$$\mathscr{W}_2 = -\sum_{i=1}^{k}[\sigma^i(\mathbf{v}_{A^i}\cdot\hat{\mathbf{t}}^i)]_{A^i} - \sum_{i=1}^{k}[\xi^i v_n^i + \mathbf{s}^i\cdot(\langle\dot{\mathbf{y}}\rangle + v_n^i\langle\mathbf{F}\rangle\hat{\mathbf{n}}^i)]_{A^i} \quad (4.28)$$

where we have used the identities (4.11) and $\mathbf{v}_{A^i} = v_n^i\hat{\mathbf{n}}^i + (\mathbf{v}_{A^i}\cdot\hat{\mathbf{t}}^i)\hat{\mathbf{t}}^i$. Then, using the divergence theorem (A8) on the second term of (4.28), we get

$$\begin{aligned}\mathscr{W}_2 = {} & -\sum_{i=1}^{k}[\sigma^i(\mathbf{v}_{A^i}\cdot\hat{\mathbf{t}}^i)]_{A^i} - \sum_{i=1}^{k}[\xi^i v_n^i + \mathbf{s}^i\cdot(\langle\dot{\mathbf{y}}\rangle + \mathbf{v}_n^i\langle\mathbf{F}\rangle\hat{\mathbf{n}}^i)]_J \\ & + \sum_{i=1}^{k}\int_{\Sigma_D^i}[\mathbf{s}^i\cdot(\mathbf{p}^i)^0 + \xi^i(\theta^i)^0]\,\mathrm{d}l + \sum_{i=1}^{k}\int_{\Sigma_D^i}\frac{\partial\mathbf{s}^i}{\partial\alpha^i}\cdot\langle\dot{\mathbf{y}}\rangle\,\mathrm{d}l \\ & + \sum_{i=1}^{k}\int_{\Sigma_D^i}\left[\frac{\partial\xi^i}{\partial\alpha^i} - \kappa^i(\bar{\mathbf{F}}^i)^T\mathbf{s}^i\cdot\hat{\mathbf{t}}^i + \frac{\partial\mathbf{s}^i}{\partial\alpha^i}\cdot\langle\mathbf{F}\rangle\hat{\mathbf{n}}^i\right]v_n^i\,\mathrm{d}l. \end{aligned} \quad (4.29)$$

Here, we have used the following identities for the normal time derivative (Appendix B) of the tangential stretch and the crystallographic direction (Gurtin, 1993):

$$(\mathbf{p}^i)^0 = \frac{\partial}{\partial\alpha^i}(\langle\dot{\mathbf{y}}\rangle + \langle\mathbf{F}\rangle v_n^i\hat{\mathbf{n}}^i) + \kappa^i v_n^i\bar{\mathbf{F}}^i\hat{\mathbf{t}}^i \quad \text{and} \quad (\theta^i)^0 = \frac{\partial v_n^i}{\partial\alpha^i}. \quad (4.30)$$

$(a^i)^0$ denotes the normal time derivative of quantity a^i following the interface Σ^i.

Finally, substituting (4.27) and (4.29) in (4.21), and using the balance law (4.15), we obtain

$$\begin{aligned}\mathscr{W}(\mathscr{D}_t) = {} & \int_{\mathscr{D}_t}\mathbf{S}\cdot\dot{\mathbf{F}}\,\mathrm{d}a + \int_{\partial\mathscr{D}_t}\pi u_m\,\mathrm{d}l - \sum_{i=1}^{k}[\sigma^i(\mathbf{v}_{A^i}\cdot\hat{\mathbf{t}}^i)]_{A^i} \\ & + \sum_{i=1}^{k}\int_{\Sigma_D^i}[\mathbf{s}^i\cdot(\mathbf{p}^i)^0 + \xi^i(\theta^i)^0]\,\mathrm{d}l \\ & + \sum_{i=1}^{k}\int_{\Sigma_D^i}\left[\frac{\partial\xi^i}{\partial\alpha^i} - \kappa^i(\bar{\mathbf{F}}^i)^T\mathbf{s}^i\cdot\hat{\mathbf{t}}^i - [\![\mathbf{S}\hat{\mathbf{n}}^i\cdot\mathbf{F}\hat{\mathbf{n}}^i]\!]\right]v_n^i\,\mathrm{d}l \\ & + \lim_{r\to 0}\int_{\partial\mathscr{B}_r}\mathbf{S}\hat{\mathbf{m}}\cdot\dot{\mathbf{y}}\,\mathrm{d}l - \sum_{i=1}^{k}[\mathbf{s}^i\cdot(\langle\dot{\mathbf{y}}\rangle + v_n^i\langle\mathbf{F}\rangle\hat{\mathbf{n}}^i) + \xi^i v_n^i]_J. \end{aligned} \quad (4.31)$$

Energy. Let the bulk energy per unit reference volume be ϕ and the interface energy per unit reference area of the interface Σ^i be ψ^i. Then the energy of the region $\mathscr{D}_t$ is

$$\mathscr{E}(\mathscr{D}_t) = \int_{\mathscr{D}_t} \phi \, \mathrm{d}a + \sum_{i=1}^{k} \int_{\Sigma_D^i} \psi^i \, \mathrm{d}l. \tag{4.32}$$

The bulk energy can be singular at the junction. Hence, we use the transport identities (A3) and (A7) to calculate the derivative of the energy (4.32) as

$$\frac{\mathrm{d}\mathscr{E}(\mathscr{D}_t)}{\mathrm{d}t} = \int_{\mathscr{D}_t} \dot{\phi} \, \mathrm{d}a + \int_{\partial\mathscr{D}_t} \phi u_m \, \mathrm{d}l - \sum_{i=1}^{k} [\psi^i \mathbf{v}_{A^i} \cdot \hat{\mathbf{t}}^i]_{A^i} + \sum_{i=1}^{k} \int_{\Sigma_D^i} \{(\psi^i)^0 - (\llbracket \phi \rrbracket + \psi^i \kappa^i) v_n^i\} \, \mathrm{d}l$$
$$- \lim_{r \to 0} \int_{\partial\mathscr{B}_r} \phi \tilde{u}_m \, \mathrm{d}l + \sum_{i=1}^{k} [\psi^i \hat{\mathbf{t}}^i \cdot \mathbf{v}_J]_J \tag{4.33}$$

where $\tilde{u}_m$ is the reference normal velocity of the circle $\partial\mathscr{B}_r$ (Fig. 6).

Dissipation inequality. In this mechanical setting, the appropriate statement of the second law of thermodynamics is the dissipation inequality

$$\Gamma(\mathscr{D}_t) \geqslant 0 \quad \text{for every } \mathscr{D}_t \subset \Omega \quad \text{where } \Gamma(\mathscr{D}_t) = \mathscr{W}(\mathscr{D}_t) - \frac{\mathrm{d}\mathscr{E}(\mathscr{D}_t)}{\mathrm{d}t}. \tag{4.34}$$

The dissipation $\Gamma(\mathscr{D}_t)$, upon using eqns (4.31) and (4.33), is

$$\Gamma(\mathscr{D}_t) = \int_{\partial\mathscr{D}_t} (\pi - \phi) u_m \, \mathrm{d}l - \sum_{i=1}^{k} [(\sigma^i - \psi^i) \mathbf{v}_{A^i} \cdot \hat{\mathbf{t}}^i]_{A^i} + \Gamma_1 + \Gamma_2 + \int_{\mathscr{D}_t} \{\mathbf{S} \cdot \dot{\mathbf{F}} - \dot{\phi}\} \, \mathrm{d}a$$
$$- \sum_{i=1}^{k} \int_{\Sigma_D^i} \{(\psi^i)^0 - \mathbf{s}^i \cdot (\mathbf{p}^i)^0 - \xi^i (\theta^i)^0\} \, \mathrm{d}l$$

where

$$\Gamma_1 \overset{\text{def}}{=} \sum_{i=1}^{k} \int_{\Sigma_D^i} \left\{ \llbracket \phi - \mathbf{S}\hat{\mathbf{n}}^i \cdot \mathbf{F}\hat{\mathbf{n}}^i \rrbracket + (\psi^i - \mathbf{s}^i \cdot \bar{\mathbf{F}}^i \hat{\mathbf{t}}^i) \kappa^i + \frac{\partial \xi^i}{\partial \alpha^i} \right\} v_n^i \, \mathrm{d}l \tag{4.36}$$

$$\Gamma_2 \overset{\text{def}}{=} \lim_{r \to 0} \int_{\partial\mathscr{B}_r} [\phi \tilde{u}_m + \mathbf{S}\hat{\mathbf{m}} \cdot \dot{\mathbf{y}}] \, \mathrm{d}l - \sum_{i=1}^{k} [\mathbf{s}^i \cdot (\langle \dot{\mathbf{y}} \rangle + v_n^i \langle \mathbf{F} \rangle \hat{\mathbf{n}}^i) + \xi^i v_n^i + \psi^i \mathbf{v}_J \cdot \hat{\mathbf{t}}^i]_J. \tag{4.37}$$

We consider a second region $\mathscr{D}_t'$ that at any given time coincides with the region $\mathscr{D}_t$, but has a different boundary velocity, i.e., $u_m' \neq u_m$. The dissipation inequality (4.34) should hold for both these regions; this requires the condition (3.16) to hold. Similarly, by considering two different regions, we can obtain two sets of boundary points (A^i) and (B^i) that coincide at a given time instant, but have different tangential velocities; the dissipation inequality (4.34) must be valid for these two choices of boundary points, which implies that

$$\sigma^i = \psi^i \quad i = 1, 2, \ldots, k. \tag{4.38}$$

Thus, the configurational stresses are

$$\mathbf{C} = \phi\mathbf{I} - \mathbf{F}^T\mathbf{S} \quad \text{in the bulk,} \tag{4.39}$$

$$\mathbf{c}^i = \psi^i\hat{\mathbf{t}}^i + \xi^i\hat{\mathbf{n}}^i - (\bar{\mathbf{F}}^i)^T\mathbf{s}^i \quad \text{on interfaces.} \tag{4.40}$$

The term $(\psi^i\hat{\mathbf{t}}^i + \xi^i\hat{\mathbf{n}}^i)$ in the interfacial configurational stress is a 90° rotation of the Cahn–Hoffman $\boldsymbol{\xi}$-vector which is given by $(\psi^i\hat{\mathbf{n}}^i - \xi^i\hat{\mathbf{t}}^i)$.

We will now simplify the terms Γ_1 (4.36) and Γ_2 (4.37); the final form of the dissipation is (4.45). Since $\xi^i = \mathbf{c}^i \cdot \hat{\mathbf{n}}^i$ [cf (4.40)], we get

$$\frac{\partial \xi^i}{\partial \alpha^i} = \frac{\partial \mathbf{c}^i}{\partial \alpha^i} \cdot \hat{\mathbf{n}}^i + \mathbf{c}^i \cdot \frac{\partial \hat{\mathbf{n}}^i}{\partial \alpha^i}.$$

Then, using (4.39) and (B1) as well as the configurational force balance (4.19), we get

$$\Gamma_1 = \sum_{i=1}^{k} \int_{\Sigma_D^i} \left[[\![\mathbf{C}]\!]\hat{\mathbf{n}}^i + \frac{\partial \mathbf{c}^i}{\partial \alpha^i} \right] \cdot \hat{\mathbf{n}}^i v_n^i \, \mathrm{d}l = -\sum_{i=1}^{k} \int_{\Sigma_D^i} \mathbf{f}_\Sigma^i \cdot \hat{\mathbf{n}}^i v_n^i \, \mathrm{d}l. \tag{4.41}$$

Next we simplify the term Γ_2. By adding and subtracting the term $\mathbf{s}^i \cdot \bar{\mathbf{F}}^i\hat{\mathbf{t}}^i(\mathbf{v}^i \cdot \hat{\mathbf{t}}^i)$ to the summation, we can rewrite the sum in (4.37) as

$$\begin{aligned} \sum_{i=1}^{k} [\cdot]|_J = &\sum_{i=1}^{k} [\mathbf{s}^i \cdot \{\langle \dot{\mathbf{y}} \rangle + \langle \mathbf{F} \rangle \hat{\mathbf{n}}^i (\mathbf{v}_J \cdot \hat{\mathbf{n}}^i) + \bar{\mathbf{F}}^i\hat{\mathbf{t}}^i (\mathbf{v}_J \cdot \hat{\mathbf{t}}^i)\}]_J \\ &+ \sum_{i=1}^{k} [(\psi^i - \mathbf{s}^i \cdot \bar{\mathbf{F}}^i\hat{\mathbf{t}}^i)(\mathbf{v}_J \cdot \hat{\mathbf{t}}^i) + \xi^i (\mathbf{v}_J \cdot \hat{\mathbf{n}}^i)]_J \\ = &\sum_{i=1}^{k} \mathbf{s}^i \cdot \{\langle \dot{\mathbf{y}} \rangle + \langle \mathbf{F} \rangle \mathbf{v}_J\}|_J + \sum_{i=1}^{k} (\mathbf{v}_J \cdot \mathbf{c}^i)|_J. \end{aligned} \tag{4.42}$$

Above, we have used the representation (4.40) and the relation $\bar{\mathbf{F}}^i\hat{\mathbf{t}}^i = \langle \mathbf{F} \rangle \hat{\mathbf{t}}^i$. Now, we add and subtract the term $\mathbf{S}\hat{\mathbf{m}} \cdot \mathbf{F}\tilde{\mathbf{u}}$ to the integrand of the integral over the circle $\partial\mathscr{B}_r$ in (4.37). Then we can rewrite Γ_2 as

$$\begin{aligned} \Gamma_2 = &\lim_{r \to 0} \int_{\partial\mathscr{B}_r} [\tilde{\mathbf{u}} \cdot (\phi\mathbf{I} - \mathbf{F}^T\mathbf{S})\hat{\mathbf{m}}] \, \mathrm{d}l - \sum_{i=1}^{k} (\mathbf{c}^i \cdot \mathbf{v}_J)|_J \\ &+ \lim_{r \to 0} \int_{\partial\mathscr{B}_r} \mathbf{S}\hat{\mathbf{m}} \cdot [\dot{\mathbf{y}} + \mathbf{F}\tilde{\mathbf{u}}] \, \mathrm{d}l - \sum_{i=1}^{k} \mathbf{s}^i \cdot (\langle \dot{\mathbf{y}} \rangle + \langle \mathbf{F} \rangle \mathbf{v}_J)|_J. \end{aligned} \tag{4.43}$$

Notice that the velocity of the circle $\partial\mathscr{B}_r$ approaches the velocity of the junction, i.e., $\tilde{\mathbf{u}} \to \mathbf{v}_J$ as $r \to 0$. Then, using the configurational force balance (4.20), we get

$$\begin{aligned} \lim_{r \to 0} \int_{\partial\mathscr{B}_r} \tilde{\mathbf{u}} \cdot \mathbf{C}\hat{\mathbf{m}} \, \mathrm{d}l - \sum_{i=1}^{k} [\mathbf{c}^i \cdot \mathbf{v}_J]_J &= \left(\lim_{r \to 0} \int_{\partial\mathscr{B}_r} \mathbf{C}\hat{\mathbf{m}} \, \mathrm{d}l - \sum_{i=1}^{k} [\mathbf{c}^i]_J \right) \cdot \mathbf{v}_J \\ &= -\mathbf{f}_J \cdot \mathbf{v}_J. \end{aligned} \tag{4.44}$$

Next we show that the sum of the last two terms of eqn (4.43) vanishes due to the balance law (4.16) using an argument similar to that of Gurtin and Podio-Guidugli (1996). Consider co-ordinates with origin at the junction and translating along with it : $\mathbf{z} = \mathbf{x} - J$ in a neighborhood of the junction J. Let us write the deformation

$$\check{\mathbf{y}}(\mathbf{z}, t) = \mathbf{y}(\mathbf{z}+J, t), \quad \text{then } \dot{\check{\mathbf{y}}} = \frac{\partial}{\partial t}\check{\mathbf{y}}(\cdot, t) = \dot{\mathbf{y}} + \mathbf{F}\mathbf{v}_J.$$

We shall assume that the deformation fields are smooth enough for $\dot{\check{\mathbf{y}}}$ to exist and for $\dot{\check{\mathbf{y}}}(\mathbf{z}, t) \to (\langle \dot{\mathbf{y}} \rangle + \langle \mathbf{F} \rangle \mathbf{v})|_J$ as $\mathbf{z} \to \mathbf{0}$ uniformly in t. The integral in the last line of the expression for the dissipation (4.43) can now be written as

$$\lim_{r\to 0} \int_{\partial \mathscr{B}_r} \mathbf{S}\hat{\mathbf{m}} \cdot \dot{\check{\mathbf{y}}} \, \mathrm{d}l$$

$$= \lim_{r\to 0} \int_{\partial \mathscr{B}_r} \mathbf{S}\hat{\mathbf{m}} \cdot ([\langle \dot{\mathbf{y}} \rangle + \langle \mathbf{F} \rangle \mathbf{v}]_J + o(r)) \, \mathrm{d}l = ([\langle \dot{\mathbf{y}} \rangle + \langle \mathbf{F} \rangle \mathbf{v}]_J) \cdot \lim_{r\to 0} \int_{\partial \mathscr{B}_r} \mathbf{S}\hat{\mathbf{m}} \, \mathrm{d}l.$$

Then the balance law (4.16) implies that the sum of the last two terms in expression (4.43) vanishes.

Putting all this together, the dissipation inequality for a region $\mathscr{D}_t \subset \Omega$ that contains a junction J is

$$\Gamma(\mathscr{D}_t) = \int_{\mathscr{D}_t} \{\mathbf{S} \cdot \dot{\mathbf{F}} - \dot{\phi}\} \, \mathrm{d}a - \sum_{i=1}^{k} \int_{\Sigma_D^i} \{(\psi^i)^0 - \mathbf{s}^i \cdot (\mathbf{p}^i)^0 - \xi^i (\theta^i)^0 + (\mathbf{f}_\Sigma^i \cdot \hat{\mathbf{n}}^i) v_n^i\} \, \mathrm{d}l - \mathbf{f}_J \cdot \mathbf{v}_J. \tag{4.45}$$

4.4. *Driving forces*

Driving forces are the forces that are conjugate to the velocities in the dissipation (4.45).

The driving force d_Σ^i on the interface Σ_i is the force conjugate to the normal interface velocity v_n^i :

$$d_\Sigma^i = -(\mathbf{f}_\Sigma^i \cdot \hat{\mathbf{n}}^i). \tag{4.46}$$

The configurational force balance (4.19), then implies that the interface driving force is

$$d_\Sigma^i = \hat{\mathbf{n}}^i \cdot [\![\phi \mathbf{I} - \mathbf{F}^T \mathbf{S}]\!] \hat{\mathbf{n}}^i + (\psi^i - (\bar{\mathbf{F}}^i)^T \mathbf{s}^i \cdot \hat{\mathbf{t}}) \kappa^i + \frac{\partial \xi^i}{\partial \alpha^i}. \tag{4.47}$$

This result was obtained in three-dimensions by Gurtin and Struthers (1990) ; also see (Eshelby, 1970 ; Larche and Cahn, 1973 ; Truskinovsky, 1982 ; Alexander and Johnson, 1985 ; Leo and Sekerka, 1989 ; Abeyaratne and Knowles, 1990 ; Gurtin and Struthers, 1990 ; Lusk, 1994 ; Gurtin, 1995).

As discussed previously, the propagation of the junction is unconstrained, whereas

the edge is constrained to move along the external boundary of the body. Hence, we consider two cases: unconstrained and constrained junctions.

Unconstrained junctions. The driving force $\mathbf{d}_J$ on an unconstrained junction J is the force conjugate to the junction velocity $\mathbf{v}_J$ in expression (4.45):

$$\mathbf{d}_J = -\mathbf{f}_J. \tag{4.48}$$

The configurational force balance (4.20) implies that the driving force on the junction is

$$\mathbf{d}_J = \lim_{r\to 0}\int_{\partial\mathscr{B}_r} (\phi\mathbf{I}-\mathbf{F}^T\mathbf{S})\hat{\mathbf{m}}\,\mathrm{d}l - \sum_{i=1}^{k}[\psi^i\hat{\mathbf{t}}^i + \xi^i\hat{\mathbf{n}}^i - (\bar{\mathbf{F}}^i)^T\mathbf{s}^i]_J. \tag{4.49}$$

Notice that this is a vector. The integral is the contribution of the bulk, while the sum is the contribution of the interfaces. The integral above is reminiscent of the J-integral of fracture mechanics. However, this integral is not path independent since the integrand can jump across interfaces. Therefore, it has meaning only in the limit $r \to 0$.

Constrained junctions or edges. As explained earlier, an edge E is viewed as a constrained triple-junction formed by an interface and the external boundary of the body. The edge E lies on the external boundary $\partial\Omega$, consequently its velocity is parallel to the tangent $\hat{\mathbf{w}}$ to the external boundary or $\mathbf{v}_J = v_E\hat{\mathbf{w}}$. Consequently, $\mathbf{f}_J\cdot\mathbf{v}_J = (\mathbf{f}_J\cdot\hat{\mathbf{w}})v_E$. Hence, we define the driving force on the edge as

$$d_E = -(\mathbf{f}_J\cdot\hat{\mathbf{w}}). \tag{4.50}$$

Again,

$$d_E = \hat{\mathbf{w}}\cdot\left[\lim_{r\to 0}\int_{\partial\mathscr{B}_r\cap\Omega}(\phi\mathbf{I}-\mathbf{F}^T\mathbf{S})\hat{\mathbf{m}}\,\mathrm{d}l + [\![\psi - \bar{\mathbf{F}}^T\mathbf{s}\cdot\hat{\mathbf{w}}]\!]\hat{\mathbf{w}} - (\psi^1 - (\bar{\mathbf{F}}^1)^T\mathbf{s}^1\cdot\hat{\mathbf{t}}^1)\hat{\mathbf{t}}^1 - \xi^1\hat{\mathbf{n}}^1\right]. \tag{4.51}$$

Notice that this is a scalar. The edge driving force contains the J-type integral and has contributions from both the interface and the boundary.

Lastly, we use the definitions of driving forces to localize the dissipation inequality and obtain

$$\Gamma_{\text{bulk}} = \mathbf{S}\cdot\dot{\mathbf{F}} - \dot{\phi} \geqslant 0 \quad \text{in}\,\Omega\backslash\Sigma(\mathrm{t}), \tag{4.52}$$

$$\Gamma_{\text{int}} = -\{\psi^0 - \mathbf{s}\cdot\mathbf{p}^0 - \xi\theta^0 - d_\Sigma v_n\} \geqslant 0 \quad \text{in}\,\Sigma(t), \tag{4.53}$$

$$\Gamma_{\text{junc}} = \mathbf{d}_J\cdot\mathbf{v}_J \geqslant 0 \quad \text{at}\,J(t), \tag{4.54}$$

$$\Gamma_{\text{edge}} = d_E(v_E) \geqslant 0 \quad \text{at}\,E(t). \tag{4.55}$$

4.5. *Constitutive equations*

We make the following constitutive assumptions

$$\text{bulk}: \quad \phi = \phi(\mathbf{F}), \quad \mathbf{S} = \mathbf{S}(\mathbf{F}); \tag{4.56}$$

$$\text{interface}: \quad \psi = \psi(\mathbf{p}, \theta), \quad \mathbf{s} = \mathbf{s}(\mathbf{p}, \theta), \quad \boldsymbol{\xi} = \boldsymbol{\xi}(\mathbf{p}, \theta). \tag{4.57}$$

The bulk is elastic. The interface is elastic and anisotropic—all interface quantities depend on the interface deformation and orientation (see Fig. 6 for the definition of θ).

Abeyaratne and Knowles (1990) have used a dissipation inequality similar to (4.53) to argue that it is necessary to provide a constitutive relation for d_Σ. Alternately, Gurtin (1995) argues that it is necessary to provide constitutive relations for the configurational forces and stresses. Following them, we appeal to (4.54) and (4.55) and argue that it is necessary to provide additional constitutive relations for $\mathbf{d}_J$ and d_E. Such constitutive relations are often called kinetic relations. We consider the following kinetic relations

$$d_\Sigma = k_\Sigma(\mathbf{p}, v_n, \theta), \quad \mathbf{d}_J = \mathbf{k}_J(\mathbf{v}_J, \theta^i), \quad d_E = k_E(v_E, \theta^i). \tag{4.58}$$

The interfacial driving force depends on the tangential stretch, the normal interfacial velocity, and crystallographic orientation. The driving force for a junction depends on both the magnitude and direction of the junction velocity as well as the limiting crystallographic orientations of the interfaces. The edge driving force depends on the magnitude of the edge velocity and the limiting crystallographic orientations.

Following Coleman and Noll (1963), we require the dissipation inequalities (4.52)–(4.55) to hold for all processes. This imposes restrictions on the constitutive assumptions (4.56)–(4.58). First, expressions (4.52) and (4.56) imply (3.20). This in turn implies that the dissipation in the bulk vanishes; $\Gamma_{\text{bulk}} = 0$.

From expressions (4.53), (4.57), and (4.58) we obtain (Gurtin and Struthers, 1990):

$$\mathbf{s} = \frac{\partial \psi}{\partial \mathbf{p}} \quad \text{and} \quad \xi = \frac{\partial \psi}{\partial \theta}. \tag{4.59}$$

Thus, the interface stress is a consequence of the tangential stretch and the interface shear of anisotropy. Consequently, the dissipation on the interface reduces to $\Gamma_{\text{int}} = d_\Sigma(\mathbf{p}, \theta, v_n) v_n$.

Now, the shear relation $(4.59)_2$ allows us to rewrite the driving forces as

$$d_\Sigma = [\![\phi]\!] - \langle \mathbf{S} \rangle \hat{\mathbf{n}} \cdot [\![\mathbf{F}]\!] \hat{\mathbf{n}} + \left(\psi + \frac{\partial^2 \psi}{\partial \theta^2} \right) \kappa - \mathbf{s} \cdot \rho \kappa + \frac{\partial^2 \psi}{\partial \rho \, \partial \theta} \frac{\partial \rho}{\partial \alpha}, \tag{4.60}$$

$$\mathbf{d}_J = \lim_{r \to 0} \int_{\partial \mathscr{B}_r} (\phi \mathbf{I} - \mathbf{F}^T \mathbf{S}) \hat{\mathbf{m}} \, \mathrm{d}l - \sum_{i=1}^{k} \left[\psi^i \hat{\mathbf{t}}^i + \frac{\partial \psi^i}{\partial \theta^i} \hat{\mathbf{n}}^i - (\bar{\mathbf{F}}^i)^T \mathbf{s}^i \right]_J,$$

$$d_E = \hat{\mathbf{w}} \cdot \left[\lim_{r \to 0} \int_{\partial \mathscr{B}_r \cap \Omega} (\phi \mathbf{I} - \mathbf{F}^T \mathbf{S}) \hat{\mathbf{m}} \, \mathrm{d}l \right. \tag{4.61}$$

$$+\left[\!\left[\psi-\mathbf{s}\cdot\bar{\mathbf{F}}\hat{\mathbf{w}}\right]\!\right]\hat{\mathbf{w}}-\psi^1\hat{\mathbf{t}}^1+(\bar{\mathbf{F}}^i)^T\mathbf{s}^1-\frac{\partial\psi^1}{\partial\theta^1}\hat{\mathbf{n}}^1\Bigg]. \tag{4.62}$$

Recall that we interpret (4.61) and (4.62) in a sense similar to (4.17).

Finally, the requirement that the dissipation inequalities (4.53), (4.54), and (4.55) hold for all evolutions of the interfaces, imposes the following restrictions on the kinetic relations:

$$k_\Sigma(\mathbf{p},v_n,\theta)v_n\geqslant 0,\quad \mathbf{k}_J(\mathbf{v}_J,\theta^i)\cdot\mathbf{v}_J\geqslant 0,\quad k_E(v_E,\theta^i)v_E\geqslant 0. \tag{4.63}$$

For example, the driving force and the velocity at an edge have the same sign (either both are positive or both are negative).

In summary, we have shown that it is necessary to prescribe constitutive relations at junctions and edges in addition to interfaces. We define driving forces and find them to be (4.60)–(4.62). These are related to the propagation velocities through the kinetic relations (4.58) which describe properties of the material. The kinetic relations satisfy the restrictions (4.63).

5. SPECIAL CASES

5.1. *Constant bulk energy*

The bulk energy is a different positive constant in each phase and the interface energies are anisotropic:

$$\phi=\text{constants};\quad \psi=\psi(\theta). \tag{5.1}$$

Hence, the bulk stress (3.20) and the interface stresses $(4.59)_1$ vanish identically, i.e. $\mathbf{S}=\mathbf{s}^i=0$. Consequently the position as well as propagation of interfaces, edges, and junctions are controlled entirely by the driving forces. The driving forces on an interface d_Σ, at a k-junction $\mathbf{d}_J$, and at an edge d_E are given by

$$d_\Sigma=\left[\!\left[\phi\right]\!\right]+\left(\psi+\frac{\partial^2\psi}{\partial\theta^2}\right)\kappa\quad\text{on }\Sigma \tag{5.2}$$

$$\mathbf{d}_J=-\sum_{i=1}^{k}\left[\psi^i\hat{\mathbf{t}}^i+\frac{\partial\psi^i}{\partial\theta^i}\hat{\mathbf{n}}^i\right]\quad\text{at } J \tag{5.3}$$

$$d_E=\left[\!\left[\psi\right]\!\right]-\psi^1(\hat{\mathbf{t}}^1\cdot\hat{\mathbf{w}})-\frac{\partial\psi^1}{\partial\theta^1}(\hat{\mathbf{n}}^1\cdot\hat{\mathbf{w}})\quad\text{at } E \tag{5.4}$$

according to (4.60)–(4.62). These driving forces are related to the respective velocities through the kinetic relations

$$d_\Sigma=k_\Sigma(v_n,\theta);\quad \mathbf{d}_J=\mathbf{k}_J(\mathbf{v}_J,\theta^i);\quad d_E=k_E(v_E,\theta^i) \tag{5.5}$$

which are subject to the restrictions (4.63). Angenent and Gurtin (1996) have obtained

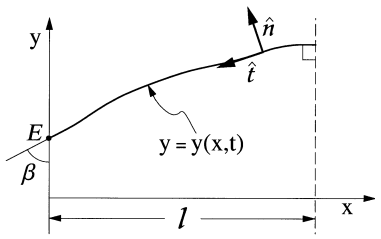

Fig. 7. The setting for the numerical example. The interface, described as $y = y(x, t)$ where $x \in (0, l)$, separates the regions Ω^+ and Ω^-; it intersects with the physical boundary ($x = 0$) at the edge E. The edge (contact) angle β is formed by the tangents to the interface and the boundary.

these results for edges and have also discussed the existence of solutions to the problem of phase boundary propagation near edges for various interfacial energies.

We now specialize to the case of isotropic interfaces (no dependence on θ^i) and the edge shown in Fig. 7. The driving force at the edge is given by $d_E = [\![\gamma]\!] + \psi \cos\beta$ where $[\![\gamma]\!]$ denotes the difference in interface energy of the boundary on two sides of the interface, ψ is the (constant) energy of the interface, and β is the edge angle formed by the tangents $\hat{\mathbf{w}}$ and $\hat{\mathbf{t}}^1$. Equilibrium corresponds to the vanishing of the driving force. This gives an equilibrium contact angle β_0 that satisfies Young's contact angle condition

$$[\![\gamma]\!] + \psi \cos\beta_0 = 0. \tag{5.6}$$

We can then rewrite the edge driving force as

$$d_E = \psi(\cos\beta - \cos\beta_0). \tag{5.7}$$

Assuming the invertibility of the kinetic relations (5.5), the evolution of the interface is determined by the equations

$$v_n = k_\Sigma^{-1}([\![\phi]\!] + \psi\kappa) \quad \text{on } \Sigma, \tag{5.8}$$

$$v_E = k_E^{-1}(\psi(\cos\beta - \cos\beta_0)) \quad \text{at } E. \tag{5.9}$$

Equation (5.8) is the well-known evolution law for isotropic interfaces in the presence of a bulk driving force and surface tension. As demonstrated in Fig. 1, eqn (5.8) alone does not determine the evolution of the interface near the edge. Equation (5.9) provides the necessary additional information. We note that Davis (1983) uses a relation of the form $v_E = f(\beta - \beta_0)$ which is consistent with (5.9) for β close to β_0.

Numerical example. Consider the interface Σ shown in Fig. 7. It is described by the equation $y = y(x, t)$. The normal velocity and curvature of the interface are given by

$$v_n = \frac{\dot{y}}{\sqrt{1 + (y')^2}} \quad \text{and} \quad \kappa = \frac{y''}{[1 + (y')^2]^{(3/2)}} \tag{5.10}$$

where the partial derivatives $\dot{y} = [\partial y(\cdot, t)/\partial t]$ and $y' = [\partial y(x, \cdot)/\partial x]$. We concentrate

on the edge E; hence we assume Nuemann or symmetry boundary conditions on the right for simplicity. We assume linear kinetics: the functions k_Σ and k_E have slopes $1/\alpha$ and $1/\delta$, respectively. We require that $\alpha \geqslant 0$ and $\delta \geqslant 0$ in order to satisfy (4.63). Finally, we take the initial position of the interface to be $y(x, 0) = 0$.

Thus, the problem of evolution is to find the function $y(x, t)$ that satisfies

$$\dot{y} = \alpha\psi\left(\frac{y''}{1+(y')^2} + \frac{[\![\phi]\!]}{\psi}\sqrt{1+(y')^2}\right), \tag{5.11}$$

$$\dot{y}(0, t) = \delta\psi(\cos\beta - \cos(\beta_0)), \tag{5.12}$$

$$y'(l, t) = 0, \tag{5.13}$$

$$y(x, 0) = 0. \tag{5.14}$$

Introducing nondimensional variables

$$z = x/l; \quad u = y/l; \quad \tau = t(\alpha\psi/l^2), \tag{5.15}$$

we rewrite the evolution eqns (5.11)–(5.14) as

$$\dot{u} = \left(\frac{u''}{1+(u')^2} + \varepsilon\sqrt{1+(u')^2}\right), \tag{5.16}$$

$$\dot{u}(0, \tau) = \frac{1}{\lambda}(\cos\beta - \cos(\beta_0)), \tag{5.17}$$

$$u'(1, \tau) = 0, \tag{5.18}$$

$$u(z, 0) = 0 \tag{5.19}$$

where

$$\varepsilon = \frac{l[\![\phi]\!]}{\psi} \quad \text{and} \quad \lambda = \frac{\alpha}{l\delta}. \tag{5.20}$$

The non-dimensional parameter ε is the ratio of bulk and interface energy contributions to the interface driving force, whereas the non-dimensional parameter λ compares the relative strengths of the interface and edge mobilities.

We take $\lambda = 0.5$, $\varepsilon = 0.1$ as well as $\beta_0 = 80^\circ$ and solve the eqns (5.16)–(5.19) using an explicit finite-difference scheme. Figure 8 shows the evolution of the interface. A

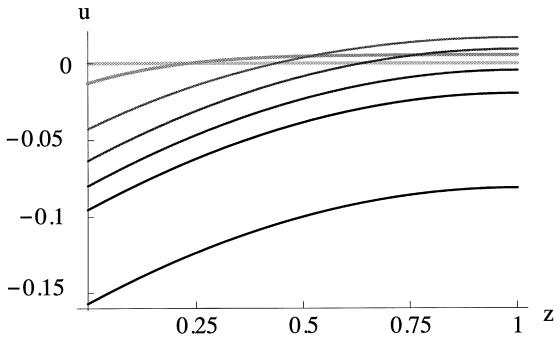

Fig. 8. Evolution of the interface for $\lambda = 0.5$, $\varepsilon = 0.1$, and $\beta_0 = 80^\circ$. The figure shows the interface at times $\tau = 0$, 100, 500, 1000, 1500, 2000, 4000; grayscale indicates increasing time.

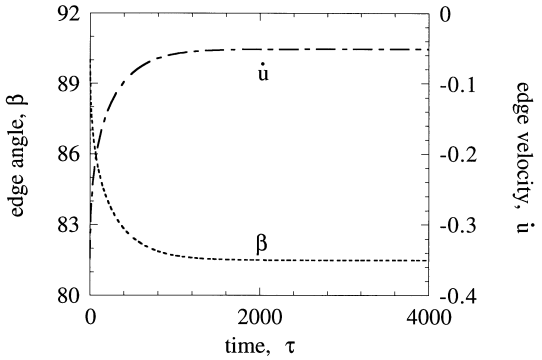

Fig. 9. The evolution of the edge angle and the edge velocity for the interface shown in Fig. 8.

positive ε tries to move the interface upwards, while the edge condition likes to rotate the edge angle from the initial value of $\beta = 90^\circ$ to the equilibrium angle of $\beta_0 = 80^\circ$. This in turn creates large curvature near the edge and that forces the interface downwards. Figure 9 shows the evolution of the edge angle and edge velocity. It is clear from both these figures that the interface is evolving towards a steady state.

Motivated by Figs 8 and 9, we look for steady state solutions of the form

$$u(z,\tau) = U(z) + v\tau. \tag{5.21}$$

The function $U(z)$ describes the steady state interface profile and v is the steady state translational velocity. Substituting (5.21) in eqns (5.16)–(5.18) and setting $w(z) = U'(z)$, we obtain

$$w' + \varepsilon(1+w^2)^{(3/2)} - v(1+w^2) = 0, \tag{5.22}$$

$$w(0) = \frac{\lambda v + \cos\beta_0}{\sqrt{1-(\lambda v - \cos\beta_0)^2}}, \tag{5.23}$$

$$w(1) = 0. \tag{5.24}$$

Above, we have expressed $\cos\beta$ in terms of w. This is a first order ordinary differential equation with an unknown coefficient v and two boundary conditions. We solve it by direct integration. The results are shown in Figs 10 and 11 for different values of the parameters λ and ε. In particular, notice the effect of the edge mobility δ: if we hold all quantities constant, then λ goes from 0 to ∞ as δ goes from ∞ to 0. An extremely mobile edge corresponds to $\delta \to \infty$ or $\lambda \to 0$. In this situation, the edge angle is always equal to equilibrium angle—see Fig. 11(a). Thus, equilibrium edge condition is obtained in the limit of infinite edge mobility. At the other limit, $\delta \to 0$ or $\lambda \to \infty$, the interface is extremely sluggish and the steady state velocity approaches zero—see Fig. 10(b).

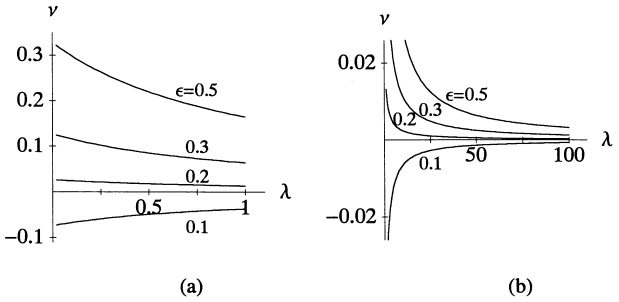

Fig. 10. Steady state translational velocity vs the ratio of interface to edge mobilities λ for (a) $\lambda < 1$ and (b) $\lambda < 100$. The velocity approaches zero for large λ (sticky edge).

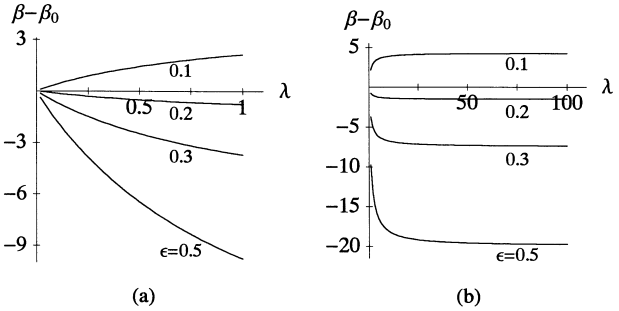

Fig. 11. Steady state edge angle vs the ratio of interface to edge mobilities λ for (a) $\lambda < 1$ and (b) $\lambda < 100$. The edge angle approaches the equilibrium value β_0 for small λ (mobile edge).

5.2. *Zero interface energy*

We neglect all surface effects and consider only bulk elastic energy, i.e.

$$\phi = \phi(\mathbf{F}); \quad \psi = 0. \tag{5.25}$$

The driving forces are then given by

$$d_\Sigma = [\![\phi]\!] - \langle \mathbf{S} \rangle \hat{\mathbf{n}} \cdot [\![\mathbf{F}]\!] \hat{\mathbf{n}} \quad \text{on } \Sigma \tag{5.26}$$

$$\mathbf{d}_J = \lim_{\eta \to 0} \int_{\partial \mathscr{B}_\eta} (\phi \mathbf{I} - \mathbf{F}^T \mathbf{S}) \hat{\mathbf{m}} \, \mathrm{d}l \quad \text{at } J \tag{5.27}$$

$$d_E = \hat{\mathbf{w}} \cdot \lim_{\eta \to 0} \int_{\partial \mathscr{B}_\eta} (\phi \mathbf{I} - \mathbf{F}^T \mathbf{S}) \hat{\mathbf{m}} \, \mathrm{d}l \quad \text{at } E \tag{5.28}$$

according to (4.60)–(4.62). The interface driving force is standard (Eshelby, 1970; Larche and Cahn, 1978; Truskinovsky, 1982; Heidug and Lehner, 1985; Abeyaratne

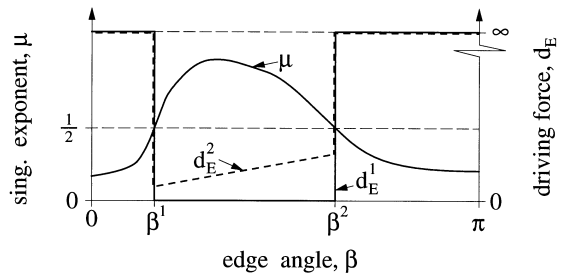

Fig. 12. A schematic figure of the order of the singularity or singular exponent μ and the driving force at the edge as a function of the edge angle β. d_E^1 is the driving force when we neglect all surface effects (Section 5.2). Notice that it is either zero or infinity except at some angles where $\mu = 1/2$ (square-root singularity). d_E^2 is the driving force when we include surface effects (Section 5.3).

and Knowles, 1990). The driving force at junctions and edges contains only the contribution to the elastic singularities and reduces to the J-type integral. These driving forces are related to the respective velocities through the kinetic relations

$$d_\Sigma = k_\Sigma(\mathbf{p}, v_n)\,; \quad \mathbf{d}_J = \mathbf{k}_J(\mathbf{v}_J)\,; \quad d_E = k_E(v_E). \tag{5.29}$$

which are subject to the restrictions (4.63).

We now discuss the consequence of these kinetic conditions on the evolution of an edge in the setting of linear elasticity. We found in Section 2.2 that the order of the singularity in the stress at a junction depends on the edge angle β and the elastic moduli of the two phases and is exactly equal to the order of the singularity in a bimaterial problem (except for isolated situations). Thus, for a fixed pair of materials (fixed pair of elastic moduli) the order μ of the singularity varies with the edge angle as shown schematically in Fig. 12. Notice that μ may be less than $1/2$ especially when we have triple junctions or edges with dissimilar anisotropic solids (Nicaise and Sändig, 1994). Recall that the displacement is of the form $\mathbf{u} \sim r^\mu f(\theta)$ and consequently the stress and strain are of the form $r^{(\mu-1)}g(\theta)$. Therefore,

$$d_E = \lim_{r\to 0} \int_0^{2\pi} r^{2(\mu-1)} h(\theta) r \,\mathrm{d}\theta = \begin{cases} \infty & 0 \leqslant \mu < \frac{1}{2} \\ d^* & \mu = \frac{1}{2} \\ 0 & \mu > \frac{1}{2} \end{cases} \tag{5.30}$$

where d^* depends on the precise state of stress. This is also shown schematically in Fig. 12 as the curve d_E^1.

Finally, let us assume that the kinetic relation is such that the edge velocity goes to infinity when the driving force does. This implies that the edge angle in any propagating interface lies between β^1 and β^2; further, the angle is either β^1 or β^2 if the edge is moving. Thus, the kinetics picks out a very special edge angle for a propagating interface. Furthermore, the dissipation at this edge is not zero, but is given by $d^* v_E$.

We conclude with a suggested experiment to study the relative importance of the

kinetics at interfaces and edges. The basic idea is to study the propagation of a single interface in specimens of different size. The dissipation has two contributions—first from the interface and second from the edges. If the applied forces in the different specimens are scaled with size so that the stress remains constant, the dissipation at the interface scales with size while the dissipation at the edges remain constant. This allows us to access the relative importance of the two sources of dissipation and hence allows us to compare their contribution to kinetics.

Consider a strip $\Omega^1 = \{0 < x_1 < 1, 0 < x_2 < l\}$ of width 1 and length l with a single interface Σ^1. Suppose the interface is induced to move with some set of boundary tractions and the solution is given by the deformation and interface position

$$\mathbf{y}(\mathbf{x}, t) = \mathbf{y}^1(\mathbf{x}, t), \quad \Sigma^1 = \{\mathbf{x} = \tilde{\mathbf{x}}(\alpha, t)\} \tag{5.31}$$

where α is the arc-length. The total dissipation in the bar is given by

$$\begin{aligned} \Gamma^1 &= \int_0^{\alpha^*} d_\Sigma^1(\alpha, t) v_n^1(\alpha, t)\, \mathrm{d}\alpha + d_E^+ v_E^+ + d_E^- v_E^- \\ &= \Gamma_\Sigma^1 + \Gamma_E^1 \end{aligned} \tag{5.32}$$

where the driving forces and velocities depend on the solution (5.31). Also, "+" and "−" refer to the top and bottom edges, respectively.

Now consider the strip $\Omega^L = \{0 < z_1 < L, 0 < z_2 < lL\}$ of width L and length lL which is scaled by L compared to Ω^1. Let us assume that the applied tractions at the boundary remain unchanged. Then, the solution is given by

$$\mathbf{y}(\mathbf{z}, \tau) = \mathbf{y}^L(\mathbf{z}, \tau) = L\mathbf{y}^1(\mathbf{z}/L, \tau/L), \quad \Sigma_L = \{\mathbf{z} = L\tilde{\mathbf{x}}(\alpha/L, \tau/L)\}. \tag{5.33}$$

Notice that the deformation gradient $\mathbf{F}^L = \nabla_z \mathbf{y}^L = \nabla_x \mathbf{y}^1 = \mathbf{F}^1$ so that $\mathbf{S}^L = \mathbf{S}^1$ and $\phi^L = \phi^1$. Consequently, $d_\Sigma^L(\alpha, \tau) = d_\Sigma^1(\alpha/L, \tau/L)$ and $d_E^{\pm,L} = d_E^{\pm,1}$. Further, since we have scaled space and time equally, the velocities remain unchanged: $v_n^L(\alpha, \tau) = v_n^1(\alpha/L, \tau/L)$ and $v_E^{\pm,L} = v_E^{\pm,1}$. Therefore,

$$\begin{aligned} \Gamma^L &= \int_0^{L\alpha^*} d_\Sigma^L(\alpha, \tau) v_n^L(\alpha, \tau)\, \mathrm{d}\alpha + d_E^+ v_E^+ + d_E^- v_E^- \\ &= \int_0^{L\alpha^*} d_\Sigma^1(\alpha/L, \tau/L) v_n^1(\alpha/L, \tau/L)\, \mathrm{d}\alpha + d_E^+ v_E^+ + d_E^- v_E^- \\ &= L \int_0^{\alpha^*} d_\Sigma^1(\beta, \tau/L) v_n^1(\beta, \tau/L)\, \mathrm{d}\beta + d_E^+ v_E^+ + d_E^- v_E^- \\ &= L\Gamma_\Sigma^1 + \Gamma_E^1. \end{aligned} \tag{5.34}$$

Comparing (5.32) and (5.34) we see that the interface dissipation scales with the size of the specimen while the edge dissipation does not.

5.3. *Zero interface stress*

In this subsection we keep anisotropic interface energy, elastic bulk energy, but neglect interface stress. In other words, the interface energy does not depend on the stretch of the interface caused by the deformation. The constitutive relations, driving forces and the kinetic relations are given by

$$\phi = \phi(\mathbf{F}); \quad \psi = \psi(\theta), \tag{5.35}$$

$$d_\Sigma = [\![\phi]\!] - \langle \mathbf{S} \rangle \hat{\mathbf{n}} \cdot [\![\mathbf{F}]\!] \hat{\mathbf{n}} + \left(\psi + \frac{\partial^2 \psi}{\partial \theta^2} \right) \kappa \quad \text{on } \Sigma, \tag{5.36}$$

$$\mathbf{d}_J = \lim_{\eta \to 0} \int_{\partial \mathscr{B}_\eta} (\phi \mathbf{I} - \mathbf{F}^T \mathbf{S}) \hat{\mathbf{m}} \, \mathrm{d}l - \sum_{i=1}^{k} \left(\psi^i \hat{\mathbf{t}}^i + \frac{\partial \psi^i}{\partial \theta^i} \hat{\mathbf{n}}^i \right) \quad \text{at } J, \tag{5.37}$$

$$d_E = \hat{\mathbf{w}} \cdot \left[\lim_{\eta \to 0} \int_{\partial \mathscr{B}_\eta \cap \Omega} (\phi \mathbf{I} - \mathbf{F}^T \mathbf{S}) \mathbf{m} \, \mathrm{d}l + [\![\psi]\!] \hat{\mathbf{w}} - \psi^1 \hat{\mathbf{t}}^1 - \frac{\partial \psi^1}{\partial \theta^1} \hat{\mathbf{n}}^1 \right] \quad \text{at } E, \tag{5.38}$$

$$d_\Sigma = k_\Sigma(\theta, v_n); \quad \mathbf{d}_J = \mathbf{k}_J(\theta^i, \mathbf{v}_J); \quad d_E = k_E(\theta^i, v_E). \tag{5.39}$$

Let us now specialize to the case of an edge in a linear elastic setting. It is easy to conclude following the discussion in Section 5.2 that the driving force at the edge is of the form shown schematically as d_E^2 in Fig. 12 since we have to add the contribution of interface energy to d_E^1.

6. GENERALIZATION TO THREE DIMENSIONS

The results derived in Section 4 can be generalized to a body in three dimensions. The following is a brief report of the main result, an expression for the driving force on a junction. The derivation will be presented elsewhere (Simha *et al.*, 1998) along with applications to problems of phase boundary propagation, crack growth, and dislocation motion.

In this setting, an interface Σ is a two-dimensional surface. Consequently, the surface stress $\bar{\mathbf{S}}$ and the surface deformation gradient $\bar{\mathbf{F}}$ [which can again be defined by (4.10)] are second order tensors which map vectors tangent to the surface to vectors in three dimensions. The surface shear is a vector $\mathbf{q}$. Multiple interfaces $\Sigma^1, \Sigma^2, \ldots, \Sigma^k$ meet at a junction J which is now a one-dimensional curve. We use $\hat{\mathbf{n}}^i$ to denote the normal to the surface Σ^i and $\hat{\mathbf{w}}^i$ to denote the binormal of Σ^i at the junction J. We use $\tilde{\mathbf{t}}$, $\tilde{\mathbf{n}}$ and $\tilde{\mathbf{b}}$ to denote the tangent, the normal and the binormal, respectively, of the junction J. $\tilde{P} = \mathbf{I} - \tilde{\mathbf{t}} \otimes \tilde{\mathbf{t}}$ is the projection tensor which maps any vector to the plane

perpendicular to the tangent $\tilde{\mathbf{t}}$. The junction has a free energy per unit length χ, a curve stress $\tilde{\mathbf{s}}$, a curve deformation gradient $\tilde{\mathbf{F}}$ and a curve shear λ. Finally, $\mathscr{C}_r$ is a circle of radius r in a plane perpendicular to J and centered at J.

The driving force on the junction J is given by

$$\mathbf{d}_{\mathscr{J}} = \tilde{\mathbf{P}}\left[\lim_{r\to 0}\int_{\mathscr{C}_r}(\phi\mathbf{I}-\mathbf{F}^T\mathbf{S})\mathbf{m}\,\mathrm{d}l-\sum_{i=1}^{k}[\psi^i\hat{\mathbf{w}}^i-(\bar{\mathbf{F}}^i)^T\bar{\mathbf{S}}^i\hat{\mathbf{w}}^i+(\bar{\mathbf{q}}^i\cdot\hat{\mathbf{w}}^i)\hat{\mathbf{n}}^i]\right.$$
$$\left.+(\chi-\tilde{\mathbf{s}}\cdot\tilde{\mathbf{F}}\hat{\mathbf{t}})\tilde{\kappa}\tilde{\mathbf{n}}+\left(\frac{\partial\tilde{\lambda}_n}{\partial\alpha}-\tilde{\tau}\tilde{\lambda}_b\right)\tilde{\mathbf{n}}+\left(\frac{\partial\tilde{\lambda}_b}{\partial\alpha}+\tilde{\tau}\tilde{\lambda}_n\right)\tilde{\mathbf{b}}\right]. \quad (6.1)$$

We make two observations. First, notice that this has $(k+2)$ contributions—one from the bulk due to the singularity, one each from the k interfaces and a final one from the curve itself. Second, notice that the driving force is a vector which lies in the plane perpendicular to the junction. The tangential component of the velocity of a propagating curve has no inherent meaning; hence the driving force is indeterminate in that direction.

ACKNOWLEDGEMENTS

This work was conducted while N.K.S. held a post-doctoral position at Caltech. We are grateful to J. K. Knowles and M. E. Gurtin for their helpful suggestions and encouragement and to M. E. Gurtin for pointing out some errors in an earlier version. We thank I-wei Chen for providing us with Fig. 2. This work was supported in part by grants from NSF (CMS 9457573) and AFOSR (F49620-95-1-0109).

REFERENCES

Abeyaratne, R. and Knowles, J. K. (1990) On the driving traction acting on a surface of strain discontinuity in a continuum. *Journal of the Mechanics and Physics of Solids* **38,** 345–360.

Alexander, J. I. D. and Johnson, W. C. (1985) Thermomechanical equilibrium in solid–fluid systems with curved interfaces. *Journal of Applied Physics* **58**(2), 816–824.

Anderson, D. M. and Davis, S. H. (1995) The spreading of volatile liquid droplets on heated surfaces. *Physics of Fluids* **7,** 248–265.

Angenent, S. and Gurtin, M. E. (1996) General contact-angle conditions with and without kinetics. *Q. Appl. Math.* **LIV,** 557–569.

Bogy, D. B. (1968) Edge-bonded dissimilar orthogonal elastic wedges under normal and shear loading. *Journal of Applied Mechanics* **35,** 460–466.

Chiao, Y.-H. and Chen, I.-W. (1990) Martensitic growth in ZrO_2—an *in situ*, small particle, TEM study of a single-interface transformation. *Acta Metallurgica et Materialia* **38**(6), 1163–1174.

Coleman, B. D. and Noll, W. (1963) The thermodynamics of elastic materials with heat conduction and viscosity. *Archive for Rational Mechanics and Analysis* **13,** 167–178.

Davis, S. H. (1983) Contact-line problems in fluid mechanics. *Journal of Applied Mechanics* **50,** 977–982.

Eshelby, J. D. (1970) Energy relations and the energy-momentum tensor in continuum mech-

anics. In: *Inelastic Behavior of Solids*, ed. M. Kanninen, W. Adler, A. Rosenfield and R. Jaffee. McGraw-Hill, New York, pp. 77–115.
Gurtin, M. E. (1981) *An Introduction to Continuum Mechanics*. Academic Press.
Gurtin, M. E. (1993) *Thermomechanics of Evolving Phase Boundaries in the Plane*. Oxford Mathematical Monographs, Oxford University Press Inc., New York.
Gurtin, M. E. (1995) The nature of configurational forces. *Archive for Rational Mechanics and Analysis* **131,** 67–100.
Gurtin, M. E. and Podio-Guidugli, P. (1996) Configurational forces and the basic laws for crack propagation. *Journal of the Mechanics and Physics of Solids* **44**(6), 905–927.
Gurtin, M. E. and Struthers, A. (1990) Multiphase thermomechanics with interfacial structure: 3. evolving phase boundaries in the presence of bulk deformation. *Archive for Rational Mechanics and Analysis* **112,** 97–160.
Gurtin, M. E. and Voorhees, P. W. (1998) On the effects of elastic stress on the motion of fully faceted interfaces. *Acta Materialia* **46,** 2103–2112.
Heidug, W. and Lehner, F. K. (1985) Thermodynamics of coherent phase transformations in non-hydrostatically stressed solids. *Pure and Applied Geophysics* **123,** 91–98.
Hoffman, R. L. (1975) A study of the advancing interface: I. interface shape in liquid–gas systems. *Journal of Colloid Interface Science* **50,** 228–241.
Kondratiev, V. A. (1967) Boundary value problems for elliptic equations in domains with conical or angular points. *Trans. Moscow Math. Soc.* **16,** 227–313.
Larche, F. and Cahn, J. W. (1973) A linear theory of thermochemical equilibrium of solids under stress. *Acta Metallurgica* **21,** 1051–1063.
Larche, F. and Cahn, J. W. (1978) Thermomechanical equilibrium of multiphase solids under stress. *Acta Metallurgica* **26,** 1579–1589.
Leguillon, D. and Sanchez-Palencia, E. (1987) *Computation of Singular Solutions in Elliptic Problems and Elasticity*. Masson, Paris and John Wiley and Sons, Chichester.
Leo, P. H. and Sekerka, R. F. (1989) The effect of surface stress on crystal–melt and crystal–crystal equilibrium. *Acta Metallurgica* **37**(12), 3119–3138.
Lusk, M. (1994) Martensitic phase transitions with surface effects. *J. Elasticity* **34,** 191–227.
Mullins, W. W. (1956) Two-dimensional motion of idealized grain boundaries. *Journal of Applied Physics* **27,** 900–904.
Murr, L. E. (1975) *Interfacial Phenomena in Metals and Alloys*. Addison-Wesley Publishing Company, Reading, U.S.A.
Nicaise, S. and Sändig, A. (1994) General interface problems—I. *Mathematical Methods in the Applied Sciences* **17,** 395–429.
Pitteri, M. (1988) On 1- and 3-D models in "non-convex" elasticity. In: *Material Instabilities in Continuum Mechanics and Related Mathematical Problems*. Clarendon Press, Oxford, pp. 395–425.
Reitich, F. and Soner, H. M. (1996) Three-phase boundary motions under constant velocities. I: The vanishing surface tension limit. *Proceedings of the Royal Society of Edinburgh A* **126,** 837–865.
Simha, N. K. and Bhattacharya, K. (1997) Equilibrium conditions at corners and edges of a phase boundary in a multi-phase solid. *Materials Science and Engineering A* **238,** 32–41.
Simha, N. K., Shenoy, V. B. and Bhattacharya, K. (1998) Kinetics of a singular curve in a three-dimensional body with applications to phase boundary propagation, crack growth and dislocation motion, in preparation.
Taylor, J. (1995) The motion of multi-phase junctions under prescribed phase-boundary velocities. *Journal of Differential Equations* **119,** 109–136.
Truskinovsky, L. (1982) Equilibrium interphase boundaries. *Dokl. Akad. Nauk. SSSR* **275**(2), 306–310.
Truskinovsky, L. (1987) Dynamics of nonequilibrium phase boundaries in a heat conducting nonlinear elastic medium. *J. Appl. Math. Mech.* (*PMM*) **51,** 777–784.

Williams, M. L. (1952) Stress singularities resulting from various boundary conditions in angular corners of plates in extension. *Journal of Applied Mechanics* **19,** 526–528.

APPENDIX A : INTEGRAL IDENTITIES

Area integrals

Consider an evolving region $\mathscr{D}_t \subset \mathbb{R}^2$ that is separated into k subregions $\mathscr{D}_t^i$ by the k evolving interfaces Σ_D^i, $i = 1, 2, \ldots, k$ (see Fig. 6). The interfaces meet at the junction J. We consider fields which are smooth in $\mathscr{D}_t^i$, but which can jump across the interfaces Σ_D^i and are singular at the junction J. We interpret the integral of a scalar field ϕ as

$$\int_{\mathscr{D}_t} \phi \, \mathrm{d}a = \lim_{r \to 0} \int_{\mathscr{D}_t \setminus \mathscr{B}_r} \phi \, \mathrm{d}a. \tag{A1}$$

Here $\mathscr{B}_r$ is a disk of radius r and center J.

Then, using classical transport identities (Gurtin, 1981),

$$\begin{aligned}
\frac{\mathrm{d}}{\mathrm{d}t} \int_{\mathscr{D}_t \setminus \mathscr{B}_r} \phi \, \mathrm{d}a &= \sum_{i=1}^{k} \frac{\mathrm{d}}{\mathrm{d}t} \int_{\mathscr{D}_t^i \setminus \mathscr{B}_r} \phi \, \mathrm{d}a \\
&= \sum_{i=1}^{k} \left[\int_{\mathscr{D}_t^i \setminus \mathscr{B}_r} \dot{\phi} \, \mathrm{d}a + \int_{\partial \mathscr{D}_t^i} \phi (\mathbf{u} \cdot \hat{\mathbf{m}}) \, \mathrm{d}l \right. \\
&\quad \left. - \int_{\Sigma_D^i \setminus \mathscr{B}_r} [\![\phi]\!] v_n^i \, \mathrm{d}l - \int_{\partial \mathscr{B}_r \cap \mathscr{D}_t^i} \phi (\tilde{\mathbf{u}} \cdot \hat{\mathbf{m}}) \, \mathrm{d}l \right] \\
&= \int_{\mathscr{D}_t \setminus \mathscr{B}_r} \dot{\phi} \, \mathrm{d}a + \int_{\partial \mathscr{D}_t} \phi (\mathbf{u} \cdot \hat{\mathbf{m}}) \, \mathrm{d}l \\
&\quad - \sum_{i=1}^{k} \int_{\Sigma_D^i \setminus \mathscr{B}_r} [\![\phi]\!] v_n^i \, \mathrm{d}l - \int_{\partial \mathscr{B}_r \cap \mathscr{D}_t} \phi (\tilde{\mathbf{u}} \cdot \hat{\mathbf{m}}) \, \mathrm{d}l.
\end{aligned} \tag{A2}$$

v_n^i is the normal velocity of interface Σ_D^i, $[\![\cdot]\!]$ denotes the jump across the interface, the boundary of the evolving region $\partial \mathscr{D}_t$ moves with a velocity $\mathbf{u}$, the boundary of the disk $\partial \mathscr{B}_r$ moves with a velocity $\tilde{\mathbf{u}}$ and the outward normals to the boundaries of the evolving region and the disk are denoted by $\hat{\mathbf{m}}$. Assuming that the smoothness of ϕ allows us to switch the differentiation and the limit $r \to 0$, we obtain a transport identity for an area integral as follows (also see Gurtin and Podio-Guidugli, 1996)

$$\begin{aligned}
\frac{\mathrm{d}}{\mathrm{d}t} \int_{\mathscr{D}_t} \phi \, \mathrm{d}a &= \lim_{r \to 0} \left[\frac{\mathrm{d}}{\mathrm{d}t} \int_{\mathscr{D}_t \setminus \mathscr{B}_r} \phi \, \mathrm{d}a \right] \\
&= \int_{\mathscr{D}_t} \dot{\phi} \, \mathrm{d}a + \int_{\partial \mathscr{D}_t} \phi (\mathbf{u} \cdot \hat{\mathbf{m}}) \, \mathrm{d}l \\
&\quad - \sum_{i=1}^{k} \int_{\Sigma_D^i} [\![\phi]\!] v_n^i \, \mathrm{d}l - \lim_{r \to 0} \int_{\partial \mathscr{B}_r} \phi (\tilde{\mathbf{u}} \cdot \hat{\mathbf{m}}) \, \mathrm{d}l.
\end{aligned} \tag{A3}$$

Let $\mathbf{a}$ be a vector field with the smoothness assumptions described above. Using the divergence theorem,

$$\int_{\mathscr{D}_t\setminus\mathscr{B}_r} \nabla\cdot\mathbf{a}\,\mathrm{d}a = \sum_{i=1}^{k}\int_{\mathscr{D}_t^i\setminus\mathscr{B}_r} \nabla\cdot\mathbf{a}\,\mathrm{d}a$$
$$= \sum_{i=1}^{k}\left[\int_{\partial\mathscr{D}_t^i}\mathbf{a}\cdot\hat{\mathbf{m}}\,\mathrm{d}l - \int_{\Sigma_D^i\setminus\mathscr{B}_r}[\![\mathbf{a}]\!]\cdot\hat{\mathbf{n}}\,\mathrm{d}l - \int_{\partial\mathscr{B}_r\cap\mathscr{D}_t^i}\mathbf{a}\cdot\hat{\mathbf{m}}\,\mathrm{d}l\right]$$
$$= \int_{\partial\mathscr{D}_t}\mathbf{a}\cdot\hat{\mathbf{m}}\,\mathrm{d}l - \int_{\partial\mathscr{B}_r}\mathbf{a}\cdot\hat{\mathbf{m}}\,\mathrm{d}l - \sum_{i=1}^{k}\int_{\Sigma_D^i\setminus\mathscr{B}_r}[\![\mathbf{a}]\!]\cdot\hat{\mathbf{n}}^i\,\mathrm{d}l. \tag{A4}$$

Assuming that the smoothness of $\mathbf{a}$ allows us to switch the differentiation with the limit $r\to 0$, we obtain a divergence theorem,

$$\int_{\mathscr{D}_t}\nabla\cdot\mathbf{a}\,\mathrm{d}a = \lim_{r\to 0}\int_{\mathscr{D}_t\setminus\mathscr{B}_r}\nabla\cdot\mathbf{a}\,\mathrm{d}a$$
$$= \int_{\partial\mathscr{D}_t}\mathbf{a}\cdot\hat{\mathbf{m}}\,\mathrm{d}l - \lim_{r\to 0}\int_{\partial\mathscr{B}_r}\mathbf{a}\cdot\hat{\mathbf{m}}\,\mathrm{d}l - \sum_{i=1}^{k}\int_{\Sigma_D^i}[\![\mathbf{a}]\!]\cdot\hat{\mathbf{n}}^i\,\mathrm{d}l. \tag{A5}$$

Finally, for a tensor field $\mathbf{A}$, we set $\mathbf{a}=\mathbf{A}^T\mathbf{b}$ for some vector $\mathbf{b}$ to obtain

$$\int_{\mathscr{D}_t}\nabla\cdot\mathbf{A}\,\mathrm{d}a = \int_{\partial\mathscr{D}_t}\mathbf{A}\hat{\mathbf{m}}\,\mathrm{d}l - \lim_{r\to 0}\int_{\partial\mathscr{B}_r}\mathbf{A}\hat{\mathbf{m}}\,\mathrm{d}l - \sum_{i=1}^{k}\int_{\Sigma_D^i}[\![\mathbf{A}]\!]\hat{\mathbf{n}}^i\,\mathrm{d}l. \tag{A6}$$

Line integrals. Let ψ be a scalar field defined on the curve Σ^i. Then, the transport identity for an integral defined on a moving interface $\Sigma_D^i\subset\Sigma^i$ is (Gurtin, 1995)

$$\frac{\mathrm{d}}{\mathrm{d}t}\int_{\Sigma_D^i}\psi\,\mathrm{d}l = \int_{\Sigma_D^i}(\psi^0-\psi\kappa v_n^i)\,\mathrm{d}l + \{\psi(\tilde{\mathbf{v}}\cdot\hat{\mathbf{t}})\}_{\alpha_1}^{\alpha_2} \tag{A7}$$

where ψ^0 is the normal-time derivative of ψ following the curve Σ^i, κ is the curvature of the curve, $\hat{\mathbf{t}}$ is the tangent to the curve, $\alpha^{1,2}$ are the arclengths of the end-points, and $\tilde{\mathbf{v}}^{1,2}$ are the velocities of the end points.

Given a function $\psi=\psi(\alpha)$ where α is the arc length, the surface divergence theorem is obtained using the fundamental theorem of calculus as

$$\int_{\Sigma_D^i}\frac{\partial\psi}{\partial\alpha}\,\mathrm{d}l = \int_{\alpha_1}^{\alpha_2}\frac{\partial\psi}{\partial\alpha}\,\mathrm{d}\alpha = \psi(\alpha_2)-\psi(\alpha_1) = \{\psi\}_{\alpha_1}^{\alpha_2}. \tag{A8}$$

APPENDIX B: EVOLVING CURVES (SURFACES)

We collect some useful surface identities (Gurtin, 1993). The Frenet formulas for a curve described using arc length parameterization [see (4.1)] are

$$\frac{\partial\hat{\mathbf{n}}}{\partial\alpha} = -\kappa\hat{\mathbf{t}} \quad\text{and}\quad \frac{\partial\hat{\mathbf{t}}}{\partial\alpha} = \kappa\hat{\mathbf{n}}; \tag{B1}$$

the curvature $\kappa=(\partial\theta/\partial\alpha)$ where θ is the angle made by the normal with the horizontal (see Fig. 6).

A path $\alpha=\bar{\alpha}(t)$ is said to be a normal arc-length trajectory, if

$$\hat{\mathbf{t}}(\bar{\alpha}(t), t) \cdot \frac{\mathrm{d}\bar{\mathbf{x}}(\bar{\alpha}(t), t)}{\mathrm{d}t} = 0. \tag{B2}$$

Then, the normal-derivative φ^0 of a function $\varphi(\alpha, t)$ is defined as

$$\varphi^0 = \frac{\mathrm{d}\varphi(\bar{\alpha}(t), t)}{\mathrm{d}t}. \tag{B3}$$

The symmetry of second derivatives implies that $(\langle\nabla\mathbf{F}\rangle\hat{\mathbf{n}})\hat{\mathbf{t}} = (\langle\nabla\mathbf{F}\rangle\hat{\mathbf{t}})\hat{\mathbf{n}}$. We use this identity and the definition (B3) to obtain

$$\frac{\partial}{\partial\alpha}(\langle\dot{\mathbf{y}}\rangle + \langle\mathbf{F}\rangle v_n\hat{\mathbf{n}}) = \rho^0 - \kappa v\bar{\mathbf{F}}\hat{\mathbf{t}} \tag{B4}$$

which gives $(4.30)_1$.